JPn

Neuroscience

The Journal of Physiology

Orexin neurons are indispensable for prostaglandin E₂-induced fever and defence against environmental cooling in mice

Yoshiko Takahashi[1,2], Wei Zhang[3], Kohei Sameshima[1], Chiharu Kuroki[1,2], Ami Matsumoto[1], Jinko Sunanaga[1,2], Yu Kono[1], Takeshi Sakurai[4], Yuichi Kanmura[2] and Tomoyuki Kuwaki[1]

Departments of [1]Physiology and [2]Anesthesiology & Critical Care Medicine, Kagoshima University Graduate School of Medical & Dental Sciences, Kagoshima 890-8544, Japan

[3]Department of Surgery, University of Alabama at Birmingham, Birmingham, AL 35294-0007, USA

[4]Department of Molecular Neuroscience and Integrative Physiology, Graduate School of Medical Science, Kanazawa University, Ishikawa 920-8640, Japan

Key points

- We recently showed that orexin neurons in the hypothalamus are indispensable for stress-induced thermogenesis.
- In this study we examined whether the orexin neurons are also important for other forms of thermogenic processes, including brain prostaglandin E₂ (PGE₂) injection that mimics inflammatory fever and environmental cold exposure.
- As was the case with stress-induced thermogenesis, orexin neuron-ablated (ORX-AB) mice exhibited a blunted PGE₂-induced fever and intolerance to cold (5°C) exposure.
- Injection of retrograde tracer into the medullary raphe nucleus, where sympathetic premotor neurons regulating thermogenesis by the brown adipose tissue are located, revealed direct and indirect projection from the orexin neurons, of which the latter seemed to be preserved in the ORX-AB mice.
- These results suggest that orexin neurons are important in general thermogenic processes, and their importance is not restricted to stress-induced thermogenesis.

Abstract We recently showed using prepro-orexin knockout (ORX-KO) mice and orexin neuron-ablated (ORX-AB) mice that orexin neurons in the hypothalamus, but not orexin peptides *per se*, are indispensable for stress-induced thermogenesis. To examine whether orexin neurons are more generally involved in central thermoregulatory mechanisms, we applied other forms of thermogenic perturbations, including brain prostaglandin E₂ (PGE₂) injections which mimic inflammatory fever and environmental cold exposure, to ORX-KO mice, ORX-AB mice and their wild-type (WT) litter mates. ORX-AB mice, but not ORX-KO mice, exhibited a blunted PGE₂-induced fever and intolerance to cold (5°C) exposure, and these findings were similar to the results previously obtained with stress-induced thermogenesis. PGE₂-induced shivering was also attenuated in ORX-AB mice. Both mutants responded similarly to environmental heating (39°C). In WT and ORX-KO mice, the administration of PGE₂ and cold exposure activated orexin neurons, as revealed by increased levels of expression of c-fos. Injection of retrograde tracer into the medullary raphe nucleus revealed direct and indirect projection from the orexin neurons, of which the latter seemed to be preserved in the ORX-AB mice. In addition, we found that glutamate receptor antagonists (D-(−)-2-amino-5-phosphonopentanoic

acid and 6-cyano-7-nitroquinoxaline-2,3-dione) but not orexin receptor antagonists (SB334867 and OX2 29) successfully inhibited PGE_2-induced fever in WT mice. These results suggest that orexin neurons are important in general thermogenic processes, and their importance is not restricted to stress-induced thermogenesis. In addition, these results indicate the possible involvement of glutamate in orexin neurons implicated in PGE_2-induced fever.

Corresponding author T. Kuwaki: Department of Physiology, Kagoshima University Graduate School of Medical and Dental Sciences, Sakuragaoka 8-35-1, Kagoshima 890-8544, Japan.   Email: kuwaki@m3.kufm.kagoshima-u.ac.jp

Abbreviations ACSF, artificial cerebrospinal fluid; AMPA, 2-amino-3-(3-hydroxy-5-methyl-isoxazol-4-yl)propanoic acid; ANOVA, analysis of variance; AP5, D-(−)-2-amino-5-phosphonopentanoic acid; AUC, area under the curve; BAT, brown adipose tissue; CNQX, 6-cyano-7-nitroquinoxaline-2,3-dione; CTb, cholera toxin subunit b; DHA, dorsal hypothalamic area; EMG, electromyogram; DMH, dorsomedial hypothalamus; GFP, green fluorescent protein; LHA, lateral hypothalamic area; MHA, medial hypothalamic area; MPO, medial preoptic area; NMDA, N-methyl-D-aspartate; ORX-AB, orexin neuron-ablated; ORX-KO, orexin-knockout; PGE_2, prostaglandin E_2; WT_{AB}, wild-type littermate of the orexin neuron-ablated mice; WT_{KO}, wild-type littermate of the orexin-knockout mice.

Introduction

Central thermoregulatory pathways are composed of multiple parallel circuits that are active depending upon the causes of the thermogenesis and the output targets [brown adipose tissue (BAT), skin blood vessels and/or skeletal muscles] (Rathner *et al.* 2008; Yoshida *et al.* 2009; McAllen *et al.* 2010; Nakamura, 2011). For example, stress-induced thermogenesis is inhibited by benzodiazepines, but not by cyclooxygenase inhibitors, while lipopolysaccharide-induced fever is inhibited by cyclooxygenase inhibitors, but not by benzodiazepines (Vinkers *et al.* 2009). The responsiveness of tail blood vessels is more sensitive to core body cooling than to skin cooling, while the responsiveness of BAT is relatively more sensitive to skin cooling than to core cooling (McAllen *et al.* 2010). Inactivation of the dorsomedial hypothalamus (DMH)/dorsal hypothalamic area (DHA), which is one of the major relay nuclei of central thermoregulation (Samuels *et al.* 2004; Nakamura *et al.* 2005; Nakamura & Morrison, 2007, 2011; Morrison, 2011; Morrison & Nakamura, 2011; Tupone *et al.* 2011), attenuates BAT thermogenesis, but not skin vasoconstriction, in response to an injection of prostaglandin E_2 (PGE_2) into the pre-optic area (Rathner *et al.* 2008).

We recently showed using orexin neuron-ablated (ORX-AB) mice that orexin neurons in the hypothalamus are indispensable for stress-induced thermogenesis (Zhang *et al.* 2010). Orexin neurons are located in the lateral hypothalamic area (LHA), the perifornical area and the DMH (Elias *et al.* 1998; Peyron *et al.* 1998; Nambu *et al.* 1999), which is the thermogenic nucleus described above. However, it is currently unclear whether the orexin neurons are important for the stress-induced form of thermogenesis only or if they are more generally involved in the above-mentioned central thermoregulatory mechanisms. To research this question, we applied other forms of thermogenic perturbations,

including PGE_2 injections and cold exposure, to ORX-AB mice. We expected that orexin neurons would have a more generalised role because some orexin neurons project to the medullary raphe (Elias *et al.* 1998; Peyron *et al.* 1998; Nambu *et al.* 1999), which is a site where all of the thermogenic output pathways to the BAT, blood vessels and skeletal muscles make synaptic connections (McAllen *et al.* 2010). In addition, orexin neurons regulate the sleep/wake state (Sakurai, 2007) and thus they may affect body temperature regulation in a general way.

In addition, our previous study (Zhang *et al.* 2010) showed relatively surprising results. Stress-induced thermogenesis was attenuated in ORX-AB mice, but not in orexin-knockout (ORX-KO) mice, which lack orexin but have preserved co-localised neurotransmitter/modulator candidates, such as glutamate (Abrahamson *et al.* 2001; Rosin *et al.* 2003; Torrealba *et al.* 2003), dynorphin (Chou *et al.* 2001), galanin (Hakansson *et al.* 1999) and nitric oxide (Cheng *et al.* 2003), in the orexin neurons. These results indicated the importance of the co-localised substances in the orexin neurons but not of orexin *per se* in stress-induced thermogenesis. In fact, the existence of orexin-dependent and orexin-independent forms of thermogenesis has recently been proposed (Rusyniak *et al.* 2011). Dynorphin and glutamate may act synergistically with orexin to promote wakefulness (Arrigoni *et al.* 2010). Nevertheless, the precise role(s) of the substances co-localised with orexin are largely unknown.

The aim of the present study was to examine whether orexin and the substances co-localised in orexin neurons contribute to PGE_2-induced fever and cold defence. We hypothesised that ORX-AB mice, but not ORX-KO mice, would show attenuation of PGE_2-induced fever and cold tolerance, as was seen for handling stress-induced thermogenesis (Zhang *et al.* 2010). In addition, we examined the possible effects of pretreatment with orexin receptor antagonists and glutamate receptor antagonists in

PGE$_2$-induced fever in wild-type (WT) mice. We found, as expected, that ORX-AB but not ORX-KO mice have blunted PGE$_2$-induced febrile responses and intolerance to cold exposure. In addition, we found that glutamate receptor antagonists, but not orexin receptor antagonists, successfully inhibited PGE$_2$-induced fever. These results show the generalised importance of orexin neurons in thermogenesis, and their importance is not restricted to stress-induced thermogenesis. In addition, these results indicate the possible importance of glutamate in orexin neurons that are involved in PGE$_2$-induced fever.

Methods

Ethical approval

All experimental procedures were performed in accordance with the guiding principles for the care and use of animals in the field of physiological sciences published by the Physiological Society of Japan (2003) and approved by the Institutional Animal Use Committee at Kagoshima University.

Animals

Animals used in this study were 5- to 8-month-old male ORX-KO mice, ORX-AB mice and corresponding WT littermates (WT$_{KO}$ and WT$_{AB}$). The ORX-KO mice, which have a nuclear translocation signal plus the LacZ (also known as β-galactosidase) gene inserted into the prepro-orexin gene, do not produce orexin-A and -B (Chemelli *et al.* 1999). ORX-KO mice were maintained as heterozygotes and crossed to obtain null mutants and WT$_{KO}$ mice. In ORX-AB mice, almost all (>98%) of the orexin neurons were ablated by 4 months of age through the expression of the neurotoxin ataxin-3, under the control of the human orexin promoter (Hara *et al.* 2001). Thus, comparing the phenotypes of ORX-KO mice and ORX-AB mice allowed us to test the roles of other neurotransmitters (e.g. glutamate and dynorphin) that are produced in orexin neurons (Chou *et al.* 2001; Rosin *et al.* 2003). ORX-AB mice were also maintained as heterozygotes and crossed with C57BL/6 mice (Clea Japan Inc., Tokyo, Japan) to obtain ORX-AB mice and WT$_{AB}$. To maximise genetic homogeneity, we backcrossed the ORX-KO and ORX-AB mice with C57BL/6 mice for more than 10 generations. The genotypes of ORX-KO and ORX-AB mice were identified by PCR of DNA extracted from the tail, as has been previously reported (Terada *et al.* 2008; Zhang *et al.* 2009).

In an immunohistochemical experiment (see below), we used ORX-KO;ORX-green fluorescent protein (GFP) mice, which were the offspring from a crossing of ORX-KO mice and ORX-GFP mice. The latter expressed enhanced GFP exclusively in orexin neurons, which were under the control of the human orexin promoter (Yamanaka *et al.* 2003). ORX-KO;ORX-GFP mice do not produce orexin-A and -B but efficiently express GFP in orexin neurons. We used ORX-KO;ORX-GFP mice because the anti-LacZ staining in ORX-KO mice in our previous study (Zhang *et al.* 2010) revealed a low penetration rate (∼10%) of LacZ in orexin neurons because of an unknown reason. Enzymatic staining with 5-bromo-4-chloro-3-indolyl-β-D-galactopyranoside (X-Gal) as a substrate also revealed a low penetration rate in ORX-KO mice (our unpublished observation).

All mice were housed in a room that was maintained at 22–24°C and with lights on at 07:00 and off at 19:00 h. Mice had food and tap water available *ad libitum*. All of the animal experiments were performed in a quiet and air-conditioned (22–24°C) room from 11:00 to 17:00 h to avoid any possible influences of circadian rhythms on body temperature.

Measurement of BAT, rectal temperatures and muscle movements under anaesthesia

Mice were anaesthetised with an I.P. injection of a mixture of α-chloralose (80 mg kg^{-1}) and urethane (800 mg kg^{-1}). The adequacy of the anaesthesia was judged by the absence of the withdrawal reflex to a pinching stimulus. The animals were warmed with a heating pad (set at 33°C), and they were allowed to breath spontaneously. The animals were placed in a prone position in a stereotaxic frame (ST-7, Narishige Scientific Instrument Lab, Tokyo, Japan) so that Bregma and Lambda were on a horizontal plane. A small hole was drilled in the skull through which a glass micropipette or a microsyringe was inserted into the brain.

A thermo probe (IT-23, Physitemp Instruments, Inc., Clifton, NJ, USA) was implanted in the BAT, and the skin was sutured. Another thermo probe (RET-3) was inserted into the rectum. An electromyogram was obtained from pin electrodes attached to the nuchal muscles. After completion of surgery, at least 1 h was allowed to pass for the variables to stabilise.

Electromyography (EMG) signals were amplified ($\times$10,000, AVB-21, Nihon Kohden Corp., Tokyo, Japan) with band-pass filters (50–1000 Hz) and fed into a personal computer after analog-to-digital conversion (PowerLab, ADInstruments Pty Ltd, Bella Vista, NSW, Australia) at a sampling frequency of 4000 Hz. The EMG signals were full-wave rectified, leak integrated (time constant = 0.1 s) and standardised with the baseline value from each individual animal.

Microinjection of PGE$_2$ into the medial preoptic area

The methods used for microinjection of drugs into the brain and verification of the injection sites were the same

as those in our previous reports (Kayaba *et al.* 2003; Zhang *et al.* 2006, 2009). In brief, the glass micropipette (outside tip diameter of 20–30 μm) was attached to a stereotaxic micromanipulator and connected by silicon tubing to a pressure injector (IM-200J, Narishige Scientific). The tip of the pipette was positioned at 0.0 mm anteroposterior to the Bregma, 0.3 mm lateral to the midline and 4.9 mm ventral to the surface of the skull. While observing the fluid meniscus in the micropipette through a dissection microscope that was equipped with an ocular micrometer, a volume of 20 nl was injected by adjusting the pressure and time of the injection.

After 10 min of control recordings, artificial cerebro-spinal fluid (ACSF) and PGE$_2$ (1 mg ml^{-1} dissolved in ACSF) were sequentially administered in this order with an interval of 90 min. At the end of the experiment, the injection site was marked by injecting 20 nl of a 4% Evans blue solution through another micropipette. The animal was deeply anaesthetised with additional chloralose/urethane and transcardially perfused with 20 ml of heparin-added saline, which was followed by 20 ml of 4% formalin. The brains were removed and stored in the formalin solution for at least 2 days before sectioning. Coronal sections of 50 μm thickness were cut serially with a vibrating microslicer (D.S.K. super-microslicer, Dosaka EM, Kyoto, Japan), mounted on adhesive-coated slides (Frontier, Matsunami Glass Ind., Ltd, Osaka, Japan), and stained with 1% neutral red. The locations of the injection sites were determined according to the atlas of Paxinos & Franklin (2001).

Telemetric measurement of body temperature

With a telemetric system (Dataquest, Data Sciences International, St Paul, MN, USA), we measured abdominal temperature and locomotor activity in a freely moving mouse in its home cage. At least 7 days before the experiment, a telemetric device (TA10ETA-F10, Data Sciences International) was implanted in the abdominal cavities of mice while they were under anaesthesia with 2–3% isoflurane. Also implanted was a guide cannula (C315GS-5/2.5; Plastics One Inc., Roanoke, VA, USA) for the intracerebroventricular administration of drugs to the lateral ventricle (1 mm lateral to the Bregma, 2.5 mm deep in the skull) (Deng *et al.* 2007). The guide cannula was closed with a cannula dummy cap and firmly fixed to the skull with dental cement. An antibiotic, cephalosporin (50 mg kg^{-1}), was injected S.C. before the surgery.

After a recovery period of 1 week, PGE$_2$ (1 mg ml^{-1}) or vehicle (ACSF) was administered (2 μl) into the lateral ventricle in random order with an intermission of at least 2 days. After finishing the PGE$_2$/ACSF experiments, the animals were exposed to cold (5°C for 4 h) or hot (39°C for 1 h) environments in random order with an intermission of at least 2 days. Cold and hot exposure was achieved by putting the animal's home cage into a refrigerator and an incubator, respectively. Of 5 ORX-AB animals examined, four did not tolerate 4 h of cold exposure (see Results). After their body temperature decreased below 30°C, these animals were taken out of the refrigerator and warmed with a heating lamp immediately.

Pharmacological experiment

We used C57BL/6 mice (Clea Japan Inc.) in this experiment. The methods for anaesthesia, stereotaxic head fixing, temperature measurement and EMG recordings were the same as those described above. The only exception was that the trachea was cannulated with polyethylene tubing for artificial ventilation because some drugs may affect not only body temperature but also respiration. The animals were ventilated (Mini Vent TYPE 845, Hugo Sachs Elektronik-Harvard Apparatus GmbH, March-Hugstetten, Germany) with oxygen-enriched (∼50%) room air. The tidal volume and the frequency of the ventilator were set to 150–200 μl and 150–200 min^{-1}, respectively (Toyama *et al.* 2009). After a stabilization period of 1 h or more, 2 μl of the drug to be examined was administered with a micro-syringe from a drilled hole over the lateral ventricle. After 5 min, PGE$_2$ (1 mg ml^{-1}, 2 μl) was administered into the same ventricle with another microsyringe, and the effects on BAT temperature, rectal temperature and EMG were observed for another 90 min. Only one drug was examined in each animal.

Five drugs were examined: ACSF (pH 7.4); an orexin receptor-1-specific antagonist, SB334867 (1 mM, Tocris Bioscience, Bristol, UK); an orexin receptor-2-specific antagonist, OX2 29 (100 mM, Tocris Bioscience); an *N*-methyl-D-aspartate (NMDA)-selective glutamate receptor antagonist, D-(-)-2-amino-5-phosphonopenta-noic acid (AP5, 10 mM, Sigma-Aldrich Co., St Louis, MO, USA); and a 2-amino-3-(3-hydroxy-5-methyl-isoxazol-4-yl)propanoic acid (AMPA)/kainate-selective glutamate receptor antagonist, 6-cyano-7-nitroquin-oxaline-2,3-dione (CNQX, 10 mM, Tocris Bioscience). All drugs were dissolved in ACSF except for SB334867. SB334867 is hydrophobic and was initially dissolved in DMSO to a concentration of 350 mM (maximum soluble concentration), and the solution was then diluted with 45% (2-hydroxypropyl)-β-cyclodextrin (Encapsin, Sigma-Aldrich Co.) in ACSF to make 10 mM of SB334867. This solution was further diluted with ACSF to make 1 mM of SB334867. In our preliminary study, neither the vehicle (4.4% Encapsin–0.3% DMSO in ACSF) nor 0.3% DMSO in ACSF affected the successive PGE$_2$-induced increase in BAT temperature, while 1% DMSO did. Therefore, 1 mM was the maximum concentration of SB334867 used in the current experimental setup.

Immunohistochemistry

The activation of orexin neurons by intra-cerebroventricular injections of PGE$_2$ or by cold exposure was examined by double immunohistochemical staining for orexin and c-fos using methods that were similar to those previously reported but with minor modifications (Watanabe *et al.* 2005; Sunanaga *et al.* 2009; Zhang *et al.* 2009, 2010). In brief, 2 h after the PGE$_2$ or ACSF injections or 1 h after the cold exposure (some ORX-AB mice did not tolerate longer cold exposures, see Results), the mice were deeply anaesthetised by an I.P. injection of urethane (1.6 g kg^{-1}) and transcardially perfused with 10 mM PBS, which was followed by a fixative solution containing 4% paraformaldehyde in PBS. Brains were excised and postfixed in the same fixative solution for 48 h at 4°C. As a control for the cold exposure, brains obtained from naïve mice were also used. After cryoprotection with 30% sucrose, serial transverse frozen sections (40 μm) were cut from the brain tissue that included the hypothalamus. Every fourth section was collected and sequentially incubated with PBS containing 0.3% Triton-X and 1% normal donkey serum for 30 min, rabbit anti-c-fos antiserum (1:1000, PC-38, Merck KGaA, Darmstadt, Germany) for 1 h, biotinylated goat anti-rabbit IgG antibody (1:200, Vector Laboratories, Inc., Burlingame, CA, USA) for 1 h and goat anti-orexin antiserum (1:100, sc-8070, Santa Cruz Biotechnology, Inc., Santa Cruz, CA, USA) for 1 h at room temperature. Finally, the tissue was incubated with Alexa Fluor 488 streptavidin conjugate (1:200, Invitrogen Corp., Carlsbad, CA, USA) and Alexa Fluor 568-labelled donkey anti-goat IgG antibody (1:200, Invitrogen) for 90 min in a dark box. The sections were then mounted on glass slides, coverslipped using mounting medium with or without DAPI (Vector Laboratories) and examined with a fluorescence microscope (Biorevo BZ-8000, Keyence Corp., Osaka, Japan and LSM700, Carl Zeiss Japan, Tokyo, Japan). Images were recorded with a 48-bit digital camera (1020 × 1350 μm window). To confirm the specificity of the antibodies, sections that were incubated without primary or secondary antibody were used as negative controls for each experiment, and no signals were observed.

For ORX-KO mice that did not express orexin, we used ORX-KO;ORX-GFP mice (see Animals). Brain sections were prepared by the same method described above and incubated with a rabbit anti-c-fos antiserum. A biotin–streptavidin system was not used. Instead, an Alexa Fluor 568-labelled goat anti-rabbit IgG antibody (1:200, Invitrogen) was used.

The numbers of single-labelled (c-fos or orexin) and double-labelled (orexin plus c-fos) cells were counted on a computer screen with the assistance of count tool in Adobe Photoshop software by an experimenter who did not know the treatment (PGE$_2$/ACSF or cold/naïve). Every 4th section in an animal (six sections per mouse) was examined, as orexin neurons were distributed over a rostral–caudal distance of ∼1 mm (Sakurai *et al.* 1998). Several reports have proposed functional dichotomy of orexin neurons located in the lateral hypothalamus and those in perifornical/dorsomedial hypothalamic area (Estabrooke *et al.* 2001; Fadel *et al.* 2002; Harris *et al.* 2005; Sunanaga *et al.* 2009; Zhang *et al.* 2009). Therefore, immunoreactivity was separately counted for medial hypothalamic area (MHA) and LHA.

Retrograde labelling of the neurons projecting to the rostral raphe pallidus

A retrograde labelling experiment (Conte *et al.* 2009; Tupone *et al.* 2011) was performed to examine whether the descending neuronal pathways from the hypothalamus to the rostral raphe pallidus, a thermogenic centre in the lower brainstem (Nakamura & Morrison, 2007, 2011; Morrison, 2011; Morrison & Nakamura, 2011; Tupone *et al.* 2011), in ORX-AB mice were normally preserved. WT$_{AB}$ and ORX-AB mice ($n = 4$ each), anaesthetised with I.P. injection of ketamine (100 mg kg^{-1}) and xylazine (0.5 mg kg^{-1}), were stereotaxically injected with cholera toxin subunit b (CTb, 20 mg ml^{-1}, 50 nl) conjugated to Alexa Fluor 488 (Invitrogen) into the rostral raphe pallidus (coordinate from the Bregma: 6.6 mm caudal, 0.0 mm lateral and 6.2 mm ventral) and the pipette was left in place for 5 min. Mice were treated with analgesic (0.05 mg kg^{-1} buprenorphine, S.C.) after the drilled hole on the skull was covered with an ointment containing antibiotic bacitracin and neomycin and the skin was sutured. After 4 days, the mice were deeply anaesthetised by an injection of urethane (1.6 g kg^{-1}, I.P.) and transcardially perfused with 10 mM PBS, which was followed by a fixative solution containing 4% paraformaldehyde in PBS. Brains were excised, post-fixed, cryoprotected and thin sectioned as described above.

CTb in the hypothalamus was detected with goat anti-CTb antiserum (1:1000, List Biological, Campbell, CA, USA), biotinylated horse anti-goat IgG antibody (1:200, Vector Laboratories) and Alexa Fluor 488 streptavidin conjugate. CTb in the brainstem was detected based on fluorescence of Alexa Fluor 488 conjugated to CTb without immunostaining. Orexin was labelled with rabbit anti-orexin antiserum (1:1000, Peptide Institute, Osaka, Japan) and Alexa 568-conjugated goat anti-rabbit IgG antibody (1:200, Vector Laboratories).

BAT morphology

To examine whether the BAT in the mutant mice was normal, microscopic morphology of the BAT was studied in WT$_{KO}$, ORX-KO and ORX-AB mice ($n = 4$ each). Intra-scapular BAT was dissected after decapitation, fixed in

formalin, embedded in paraffin and thin sectioned at $4\,\mu\mathrm{m}$. Specimens were stained with haematoxylin and eosin.

Statistics

Physiological and pharmacological experimental results were assessed by analysis of variance (ANOVA) with genotype and drug as the main factor and time as a repeated measure. When appropriate, the within-subjects effects over time were determined by a Bonferroni's *post hoc* test. Response magnitude in each parameter over the time course was calculated as the area under the curve (AUC) above the baseline. To compare AUC among the groups, we used one-way ANOVA followed by Bonferroni's *post hoc* test. The immunohistochemical results were analysed by one-way ANOVA. GraphPad Prism software (GraphPad Software, Inc., La Jolla, CA, USA) was used for these calculations. Data are presented as mean $\pm$ SEM. Differences with *P* values less than 0.05 were considered significant.

Results

Eliminated PGE$_2$-induced fever in ORX-AB mice but not in ORX-KO mice

We previously showed that stress-induced thermogenesis was significantly attenuated in ORX-AB mice but not in ORX-KO mice (Zhang *et al.* 2010). Here, we examined whether the same was true for PGE$_2$-induced fever, which is a different form of thermogenic response.

There were no differences in the initial BAT temperatures or rectal temperatures among the genotypes while under chloralose/urethane anaesthesia. In WT$_{KO}$ and WT$_{AB}$ mice, BAT temperature increased by $\sim3.0^\circ$C (Fig. 1*A*), and rectal temperature increased by $\sim1.5^\circ$C (Fig. 1*B*) 30 min after a microinjection of PGE$_2$ (20 ng, ~57 pmol) into the medial preoptic area. BAT and rectal temperatures returned almost to the initial values within 70 min.

As was the case for handling stress-induced thermogenesis in our previous study, ORX-KO mice, but not ORX-AB mice, showed similar febrile responses to those in the control mice. ORX-AB mice showed no febrile response ($P = 0.44$ for BAT and $P = 0.08$ for rectum, comparison among time points by one-way ANOVA), and thus their BAT and rectal temperatures stayed within the range of the vehicle injection (Fig. 1*A'* and *B'*).

In addition, we analysed nuchal EMG as a measure of shivering. Changes in the integrated EMG by PGE$_2$ in WT$_{KO}$ and WT$_{AB}$ mice peaked earlier (Fig. 1*C*, 10–20 min after the injection) than the changes in BAT temperature and rectal temperature (30–40 min) and gradually returned to baseline values. In ORX-KO mice, changes in the integrated EMG occurred slowly (peaking

30 min after the injection), and the magnitude was smaller than that in WT$_{KO}$ ($P < 0.05$, Fig. 1*C'*). In a similar manner, changes in the integrated EMG in ORX-AB mice occurred slowly and the magnitude was smaller than that in WT$_{AB}$ ($P < 0.01$). As a whole, the PGE$_2$-induced responses were slightly blunted in ORX-KO mice and severely attenuated in ORX-AB mice.

The microinjection sites were examined after the experiment, and they were confirmed to be within the medial preoptic area (Fig. 1*D* and *E*).

### Blunted PGE$_2$-induced fever in unanesthetised ORX-AB mice

To exclude any possible interactions with the anaesthetics in the previous experiment, we used telemetric body temperature measurements in unanesthetised freely moving animals for the next step.

There was no difference in the initial abdominal temperature ($\sim36.5^\circ$C) among the genotypes, although it was higher than rectal temperatures in chloralose/urethane-anaesthetised conditions ($\sim36.0^\circ$C). In WT$_{KO}$ and WT$_{AB}$ mice, the abdominal temperature increased by $\sim3.0^\circ$C (Fig. 2*A*) at 30–40 min after an injection of PGE$_2$ (2 μg) into the lateral ventricle. Their abdominal temperature then gradually returned to the initial values over the observation period of 150 min. In ORX-KO mice, a response that was similar to those in WT$_{KO}$ and WT$_{AB}$ mice was observed. In ORX-AB mice, by contrast, abdominal temperature did not change after an injection of PGE$_2$. Although there were some perturbations in abdominal temperature, they were not significantly different from the baseline values and not different from those after vehicle injection (Fig. 2*B*). Thus, the PGE$_2$-evoked febrile response was eliminated in ORX-AB mice, but not in ORX-KO mice, in both anaesthetised and unanesthetised conditions.

Intolerance of ORX-AB mice to environmental cooling

We next examined another type of stimulation that induces thermogenesis. Mice with indwelling telemeters were put into a cold (5°C) environment. In WT$_{KO}$ and WT$_{AB}$ mice, the abdominal temperature initially decreased, reached its nadir ($\sim34^\circ$C) at around 90 min and then slightly increased towards the baseline (Fig. 3*A*). Although the abdominal temperatures never returned to the initial value during the cold exposure, it remained over 34°C and returned to the initial value after the animals were returned to room temperature (22–24°C).

In ORX-KO mice, a similar change in abdominal temperature was observed in comparison with those in WT$_{KO}$ and WT$_{AB}$ mice. However, four out of five ORX-AB mice did not tolerate 4 h of cold exposure. In particular, in three ORX-AB mice, abdominal temperature rapidly fell and reached the endpoint of 30°C within 50–150 min of
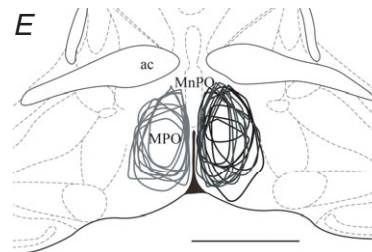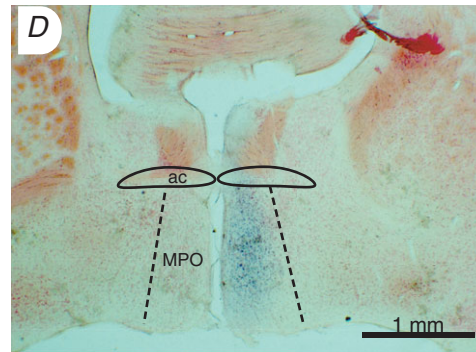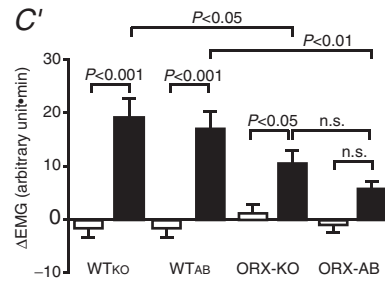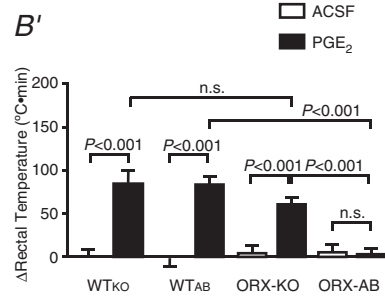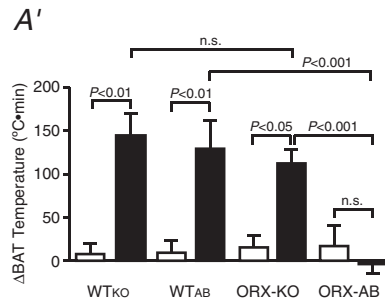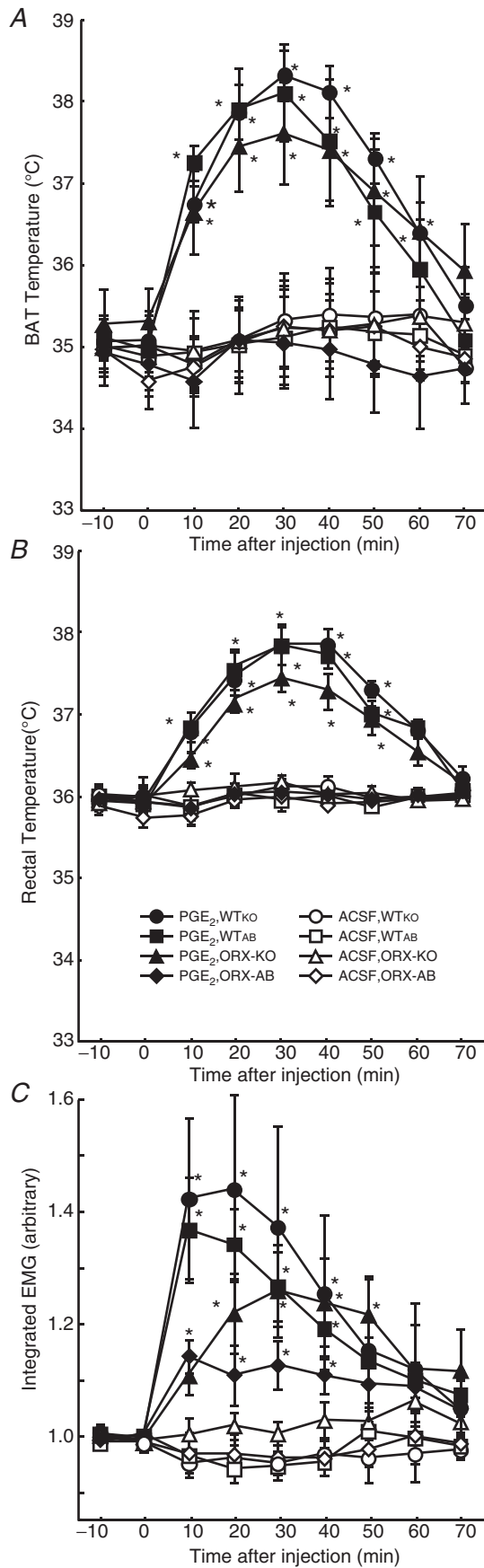
cold exposure. The magnitude of the temperature decrease in ORX-AB mice was significantly greater ($P < 0.05$) than that in WT_{AB} mice when evaluated as AUC during the initial 60 min (inset to Fig. 3*A*).

In the cold exposure experiment, we also analysed locomotor activity of the mice (Fig. 3*B*). Locomotion was increased only in the initial period of less than 30 min, and thereafter all of the mice stayed in one place in a crouching position and surrounded by wooden bedding chips. There was no difference in locomotor activity among the genotypes (inset to Fig. 3*B*). Therefore, the intolerance of the ORX-AB mice to the cold exposure cannot be explained by a defect in behavioural thermo-regulation in this mutant.

Preserved response to hot exposure in ORX-AB mice

To further examine the temperature regulation in ORX-AB mice, the animals were exposed to a hot environment (39°C). In WT_{KO} and WT_{AB} mice, the abdominal temperature increased by ~1.5°C 40 min after the heat exposure and remained at the highest value (~38°C) during the latter half of the exposure period (Fig. 4*A*). After the animals were returned to a room temperature (22–24°C) environment, abdominal temperature soon returned to the baseline and fell further below the baseline. Locomotor activity increased significantly for the initial 10 min and gradually returned to the baseline value during the entire exposure period (Fig. 4*B*).

In ORX-KO and ORX-AB mice, the changes in abdominal temperature and changes in locomotor activity in response to heat exposure compared to controls were identical with respect to the time course and magnitude.

Activation of hypothalamic neurons by PGE$_2$ and cold exposure

We next examined whether the orexin neurons and other hypothalamic neurons were activated by the intracerebroventricular administration of PGE$_2$ or by cold exposure. For this, we used immunohistochemical detection of orexin-like (in the WT_{AB} mice and the ORX-AB mice) immunoreactivity together with

that of c-fos-like immunoreactivity. In addition, we used ORX-KO;ORX-GFP mice (see Animals section for details). ORX-KO;ORX-GFP mice do not produce orexin-A and -B but efficiently and exclusively express GFP in orexin neurons. In our preliminary study, in fact, an ORX-KO heterozygous mouse which carried the ORX-GFP transgene expressed GFP in ~80% of orexin-immunopositive cells, and the ectopic expression of GFP was never observed, as was the case in WT;ORX-GFP mice (Yamanaka *et al.* 2003). An ORX-KO;ORX-GFP mouse did not show any orexin-like immunoreactivity, as expected.

After the administration of PGE$_2$ in WT_{AB} mice, the numbers of c-fos-immunopositive cells and double-labelled (orexin plus c-fos) cells in both MHA and LHA (Fig. 5*E*) were significantly larger than those observed after vehicle administration, while the total number of orexin-immunopositive cells was not different between the treatments (Fig. 5*F* and *G*). Consequently, the percentage of double-labelled cells among the orexin-positive cells was significantly higher in the brains of PGE$_2$-treated WT_{AB} mice (66.4 ± 11.7% in the medial area and 37.8 ± 7.2% in the lateral area, $n = 4$) than in vehicle-treated WT_{AB} mice (23.7 ± 7.1% in the medial area and 18.9 ± 2.4% in the lateral area, $n = 4$, $P < 0.05$).

In the ORX-KO;ORX-GFP mice, a similar result was obtained (double-labelled cells were 73.9 ± 8.2 and 44.1 ± 8.2% in the MHA and LHA, respectively, with PGE$_2$ treatment, $n = 4$ *vs.* 26.5 ± 2.3 and 23.1 ± 1.9% in the MHA and LHA, respectively, with vehicle treatment, $n = 4$, $P < 0.05$), although there was no difference in the total numbers of GFP-positive and orexin-immunopositive cells in WT_{AB} mice.

No orexin-like immunoreactivity was observed in the ORX-AB mice, as expected. Of note, the numbers of c-fos-positive cells were not increased by PGE$_2$ treatment in the MHA (Fig. 5*F*) while a comparable increase was observed in the LHA (Fig. 5*G*).

To examine the possible activation of orexin neurons by cold exposure, we used untreated naïve mice as controls, and experimental brains were excised after 1 h of cold exposure. There was no difference in the total number of

Figure 1. Effect of microinjections of PGE$_2$ into the medial preoptic area on body temperature and the EMG in mice of the four genotypes
In chloralose (80 mg kg^{-1})/urethane (800 mg kg^{-1})-anaesthetised mice, ACSF (20 nl) and PGE$_2$ (1 mg ml^{-1} in ACSF) were sequentially microinjected into the medial preoptic area (MPO) (*D*, *E*). Time-related changes in brown adipose tissue (BAT) temperature, rectal temperature and nuchal EMG (a measure of shivering) are shown in *A*, *B* and *C*, respectively, and the changes expressed as the AUC above the baseline in them for 70 min are summarized in *A'*, *B'* and *C'*, respectively. Data are presented as mean ± SEM of orexin-knockout mice (ORX-KO, $n = 6$), orexin neuron-ablated mice (ORX-AB, $n = 6$), and their corresponding wild-type littermates (WT_{KO}, $n = 4$ and WT_{AB}, $n = 5$). *E*, summary for injected sites. Left side shows dye distribution in WT_{KO} and WT_{AB} mice and right side shows that of ORX-KO and ORX-AB mice. In the actual experiment, drugs and dye were injected into unilateral MPO. *$P < 0.05$ compared with baseline values before injection (Bonferroni's *post hoc* test). n.s., Not significant. ac, Anterior commissure; MnPO, median preoptic area.

orexin-immunopositive cells (∼220 in the medial hypo-thalamic area and ∼280 in the LHA) in WT_{AB} mice and GFP-positive cells (∼200 in the medial hypothalamic area and ∼240 in the LHA) in ORX-KO;ORX-GFP mice between the cold exposure experiment (Fig. 6) and the PGE₂ experiment (Fig. 5), showing reproducible results. As was the case with PGE₂ treatment, cold exposure increased the number of c-fos-positive cells in the areas examined in the hypothalamus in both WT_{AB} mice and ORX-KO;ORX-GFP mice. Cold exposure significantly increased the percentage of double-labelled cells among the orexin- or GFP-positive cells in both WT_{AB} mice (81.3 ± 4.0 and $59.6 \pm 8.2\%$ in the MHA and LHA, respectively, $n = 4$ with cold exposure vs. 23.6 ± 5.1 and $17.7 \pm 4.0\%$ in the MHA and LHA, respectively, $n = 4$ in the controls, $P < 0.01$) and ORX-KO;ORX-GFP mice

(65.0 ± 7.1 and $52.8 \pm 4.2\%$ in the MHA and LHA, respectively, $n = 4$ with cold exposure vs. 17.6 ± 3.9 and $24.2 \pm 5.2\%$ in the MHA and LHA, respectively, $n = 4$ in the controls, $P < 0.01$).

In the ORX-AB mice, no orexin-like immunoreactivity was observed. Cold exposure increased c-fos expression in the LHA but not in the MHA (Fig. 6), which was similar to the PGE₂ experiment (Fig. 5).

The number of c-fos-positive cells in the control naïve mice brains (100–200, Fig. 6) in the cold exposure experiment was far lower than that in the vehicle-treated control mice brains in the PGE₂ experiment (400–500, Fig. 5). These results showed that injections of vehicle were somewhat stressful. However, it should be emphasised that injection of PGE₂ further increased c-fos-positive cells and double-labelled cells.
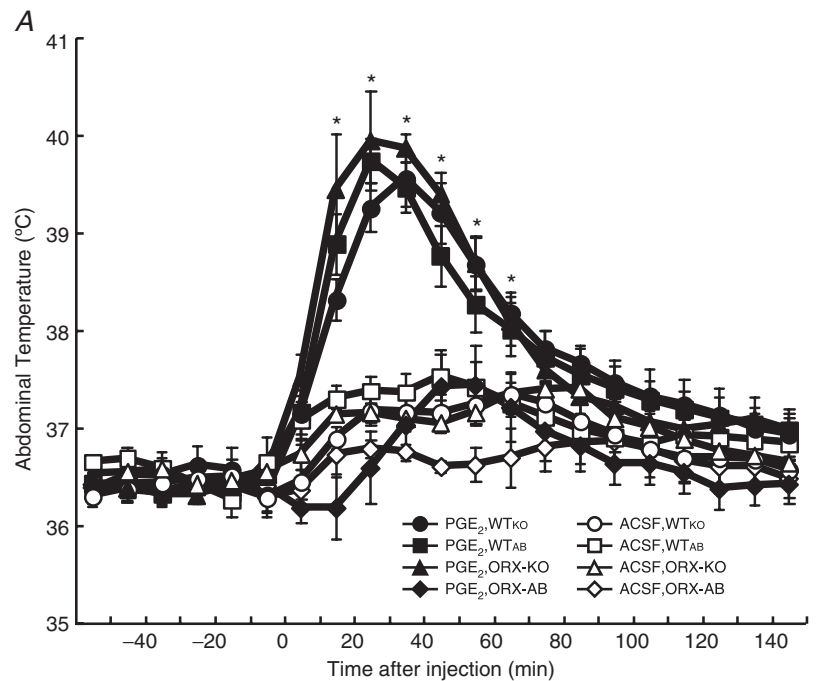

Figure 2. Effect of administration of PGE₂ into the lateral ventricle on abdominal temperature in freely moving mice with indwelling telemeters of the four genotypes
ACSF (2 μl) or PGE₂ (1 mg ml⁻¹ in ACSF) were administered through a cerebroventricular cannula in random order with an intermission of at least 2 days. Abdominal temperature was continuously monitored by a telemetric system. Time-related changes (A) and the changes expressed as the AUC above the baseline for 100 min (B) are shown. Data are presented as mean ± SEM of orexin-knockout mice (ORX-KO, $n = 8$ for PGE₂ and $n = 6$ for ACSF), orexin neuron-ablated mice (ORX-AB, $n = 8$ for PGE₂ and $n = 5$ for ACSF), and their corresponding wild-type littermates (WT_{KO}, $n = 8$ for PGE₂ and $n = 6$ for ACSF and WT_{AB}, $n = 7$ for PGE₂ and $n = 6$ for ACSF). *$P < 0.05$ compared with baseline value before injection (Bonferroni's *post hoc* test). n.s., Not significant.
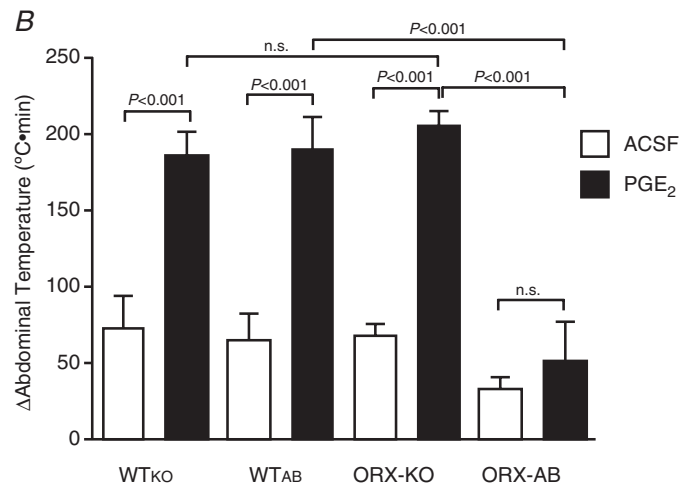
Preserved descending pathway from the hypothalamus to medullary raphe nucleus in ORX-AB mice

To examine whether the descending neuronal pathways from the hypothalamus to the rostral raphe pallidus in ORX-AB mice were normally preserved, we performed a retrograde labelling experiment. Four days after injection of CTb into the raphe pallidus (Fig. 7*B* and *E*), CTb-immunopositive cells were found in the dorsal, medial and lateral regions of the hypothalamus (Fig. 7*A*
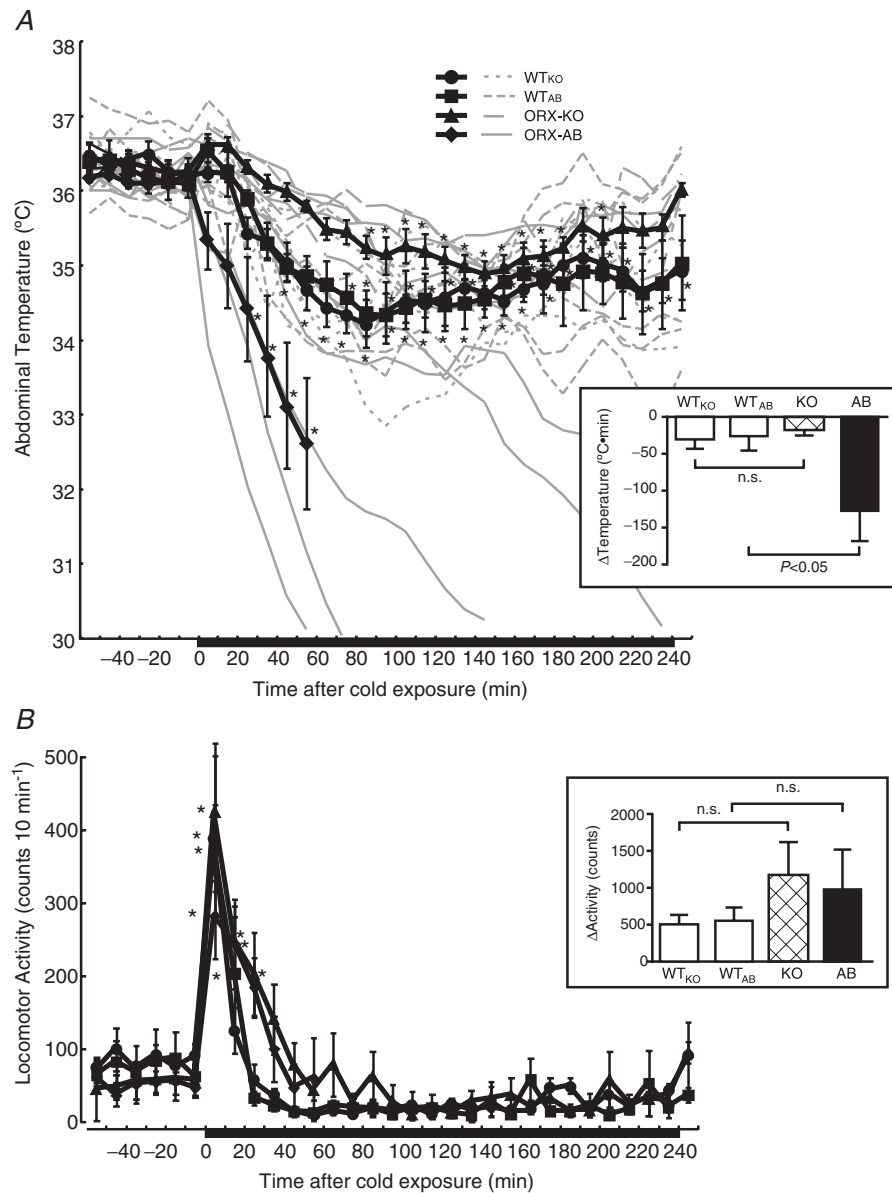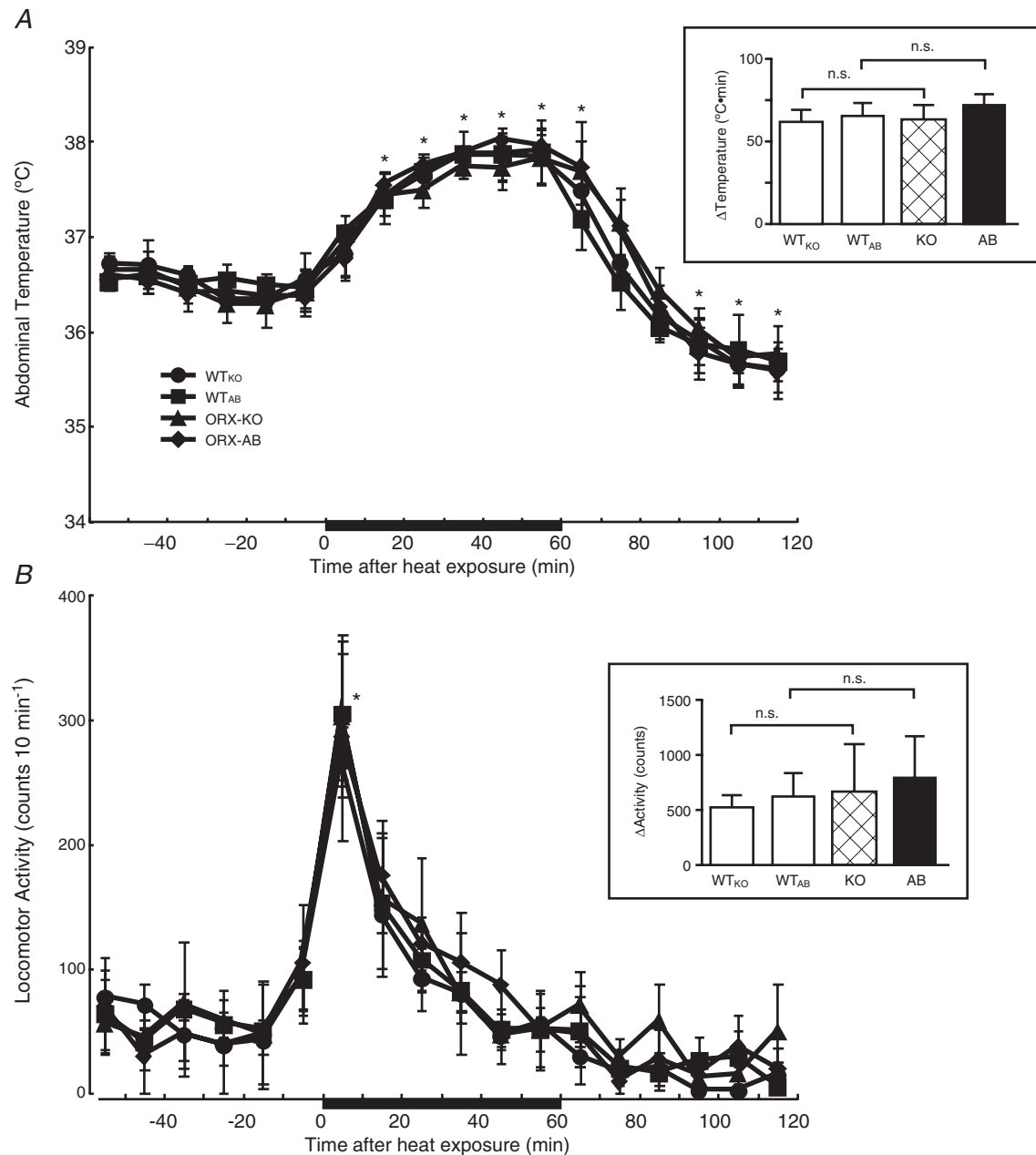

Figure 3. Effect of cold exposure on abdominal temperature and locomotor activity in freely moving mice with indwelling telemeters of the four genotypes
Mice were exposed to a cold environment (5°C) for 4 h while abdominal temperature and locomotor activity were continuously monitored by a telemetric system. When the animal's body temperature decreased below 30°C, cold exposure was terminated and the animal was immediately warmed with a heating lamp. Time-related changes in abdominal temperature (*A*) and locomotor activity (*B*) are shown. The thin grey lines indicate the data from an individual animal, and the thick black lines are the mean ± SEM ($n = 5$ in each group) of orexin-knockout mice (ORX-KO), orexin neuron-ablated mice (ORX-AB), and their corresponding wild-type littermates (WT$_{KO}$ and WT$_{AB}$). Note that only one mouse out of five ORX-AB mice tolerated the 4 h of cold exposure. Insets are the changes in the abdominal temperature and locomotor activity expressed as the AUC above the baseline. AUC was calculated for only 60 min during the initial part of the cold exposure because of the endpoint in some ORX-AB mice. *$P < 0.05$ compared with baseline value before cold exposure (Bonferroni's *post hoc* test). n.s., Not significant.

and *D*). In WT$_{AB}$ mice, the distribution of CTb-positive cells in the LHA, perifornical area, and lateral part of the DMH overlaps with the distribution of orexin neurons and many of the CTb-positive cells also expressed orexin. Outside of the distribution area of the orexin neurons, there was a cluster of CTb-positive cells in the medial part

of the DMH near the third ventricle and the DHA. Of note, some of the CTb-positive cells in the DHA seemed to be innervated by orexin-containing nerve terminals (Fig. 7*C'*).

Although orexin neurons completely disappeared in ORX-AB mice, there was no difference in the number

Figure 4. Effect of heat exposure on abdominal temperature and locomotor activity in freely moving mice with indwelling telemeters of the four genotypes
Mice were exposed to a hot environment (39°C) for 1 h while abdominal temperature and locomotor activity were continuously monitored by a telemetric system. Data are presented as mean ± SEM of orexin-knockout mice (ORX-KO, $n = 5$), orexin neuron-ablated mice (ORX-AB, $n = 5$) and their corresponding wild-type littermates (WT$_{KO}$, $n = 4$ and WT$_{AB}$, $n = 4$). Insets are the changes in the abdominal temperature and locomotor activity expressed as the AUC above the baseline calculated for 60 min of the heat exposure. *$P < 0.05$ compared with baseline values before heat exposure (Bonferroni's *post hoc* test). n.s., Not significant.
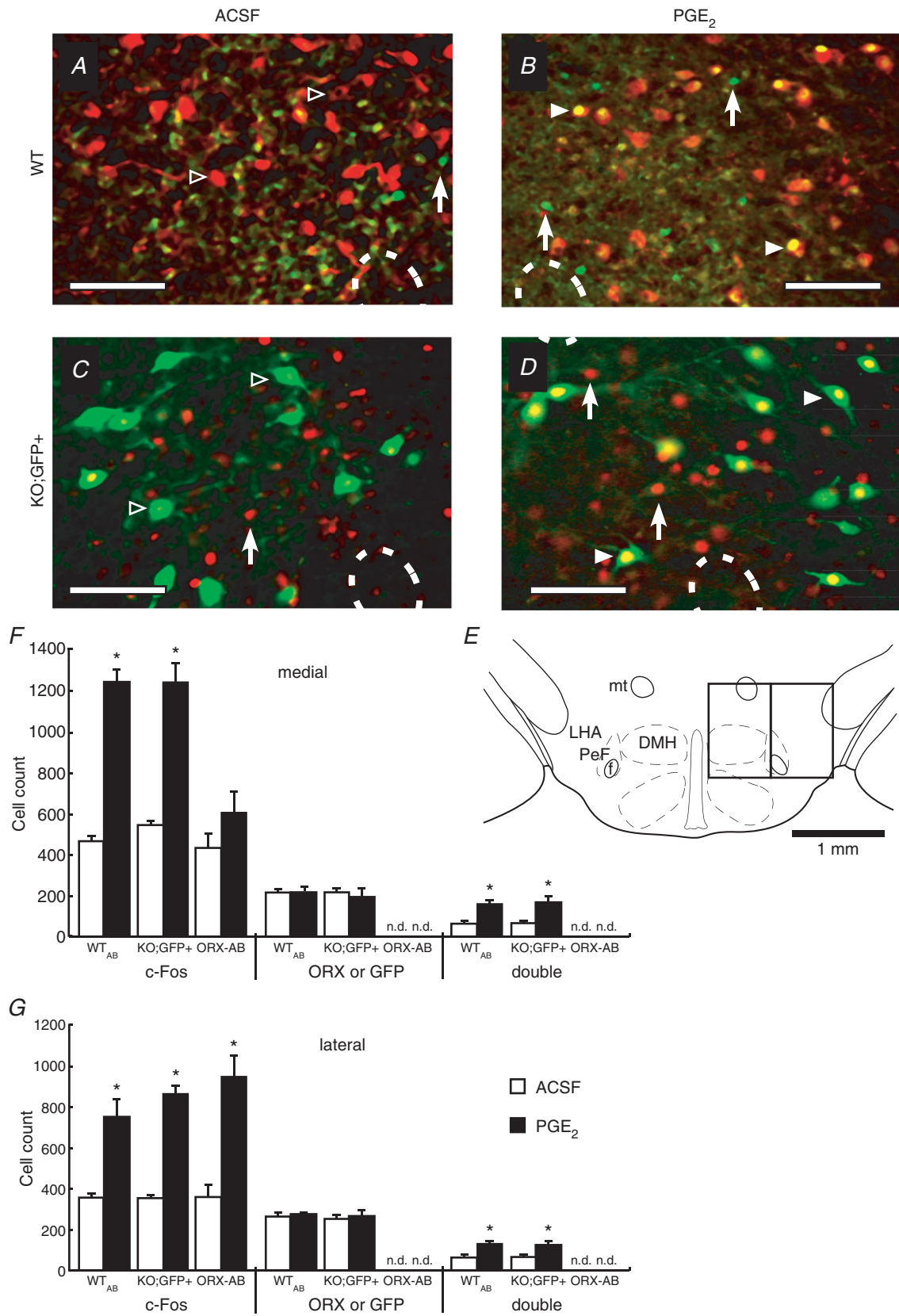
(690 ± 46 in WT$_{AB}$ vs. 653 ± 48 in ORX-AB, $n = 4$ each) or distribution of the CTb-positive cells within the hypothalamus as compared to the WT$_{AB}$ mice. Of note, a cluster of CTb-positive cells in DMH/DHA was well preserved.

Preserved BAT morphology in ORX-AB mice

To examine whether the BAT in the mutant mice was normal, microscopic morphology of the BAT was studied in WT$_{KO}$, ORX-KO and ORX-AB mice ($n = 4$ each). Intrascapular BAT was apparently normal in both ORX-KO and ORX-AB mice (Fig. 8), indicating that abnormal thermoregulation in ORX-AB cannot be attributed to abnormality of the BAT.

Attenuation of PGE$_2$-induced fever by glutamate, but not orexin, blockers

To further examine the possible neurotransmitters that are involved in PGE$_2$-induced fever, we conducted a pharmacological experiment using WT mice of the C57BL/6 strain.

In chloralose/urethane-anaesthetised mice, intracerebroventricular injections of PGE$_2$ (2 μg) increased the BAT temperature (Fig. 9A and 9A′) and rectal temperature (Fig. 9B and 9B′), as was the case in unanesthetised mice with indwelling telemeters. Increases in the temperature in this experiment (BAT by ~2°C and rectum by ~1°C) were, however, smaller than those in the unanesthetised condition (by ~3°C, see Fig. 2). Pretreatment (I.C.V.) with an orexin-1 receptor antagonist, SB334867 (2 μmol), or with an orexin-2 receptor antagonist, OX2 29 (200 μmol), did not affect the febrile effects of the subsequent injections of PGE$_2$. In contrast, I.C.V. pretreatment with an NMDA-selective

glutamate receptor antagonist, AP5 (20 μmol), and with an AMPA/kainate-selective glutamate receptor antagonist, CNQX (20 μmol), significantly inhibited the febrile effects of the subsequent injection of PGE$_2$.

In addition, we analysed nuchal EMG as a measure of shivering. In the vehicle pretreatment group after the administration of PGE$_2$, the integrated EMG rapidly increased and remained at high values during the entire observation period of 90 min (Fig. 9C). As was the case for the BAT temperature and rectal temperature, I.C.V. glutamate receptor antagonists, but not orexin receptor antagonists, significantly attenuated the increase in EMG (Fig. 9C′).

Discussion

In our previous study using ORX-KO and ORX-AB mice, we demonstrated that orexin neurons, but not orexin *per se*, are indispensable for handling stress-induced thermogenesis (Zhang *et al.* 2010). We hypothesised that the same would be true for PGE$_2$-induced fever and cold tolerance. As expected, ORX-AB, but not ORX-KO, mice showed an attenuated temperature change in response to the administration of PGE$_2$ into the medial preoptic area while mice were under chloralose/urethane-anaesthetised conditions (Fig. 1) and into the lateral ventricle while the mice were under awake and freely moving conditions (Fig. 2). The exceptional and unexpected result was that PGE$_2$-induced shivering was blunted not only in ORX-AB mice, but also in ORX-KO mice (Fig. 1). With cold exposure, body temperature in ORX-AB mice progressively decreased and reached 30°C, while body temperature in ORX-KO mice and WT mice did not decrease below 33°C (Fig. 3). The responses of body

Figure 5. Immunohistochemical evidence for the activation of orexin neurons by the administration of PGE$_2$ into the lateral ventricle
A and *B*, representative photographs of double immunostaining for orexin and c-fos in the hypothalamus of WT mice sampled 2 h after the administration of ACSF (*A*) or PGE$_2$ (*B*) into the lateral ventricle. Orexin is stained in red, c-fos in green. Yellow designates cells stained for both orexin and c-fos. Filled triangles indicate double-stained cells, and open triangles indicate orexin-containing but not c-fos-expressing cells. Arrows indicate c-fos in non-orexin cells. *C* and *D*, representative photographs of immunostaining for c-fos in the hypothalamus of orexin-knockout (KO) mice that carries the orexin neuron-specific expression of green fluorescent protein (KO;GFP+). Brains were sampled 2 h after the administration of ACSF (*C*) or PGE$_2$ (*D*) into the lateral ventricle. c-fos is stained in red. Yellow designates cells that possess GFP and are stained for c-fos. Filled triangles indicate double-labelled cells, and open triangles indicate GFP-containing but not c-fos-expressing cells. Arrows indicate c-fos in non-orexin cells. Bar = 100 μm. In *A–D*, the fornix is shown with a dashed line. *E*, schematic drawing of a coronal section of the mouse brain showing structure of the hypothalamus. The two rectangles denote examined area (1020 × 675 μm, each) for medial and lateral parts of the dorsal hypothalamus. Both sides were examined in the actual experiment although only right side windows were depicted for simplicity. DMH, dorsomedial hypothalamus; f, fornix; LHA, lateral hypothalamic area; mt, mammillothalamic tract; PeF, perifornical area. *F* and *G*, numbers of c-fos-immunopositive cells, orexin (ORX) or GFP-containing cells, and double-labelled cells (c-fos and ORX in WT, and c-fos and GFP in KO) in the medial (*F*) and lateral (*G*) part of the hypothalamus. Data are presented as the mean ± SEM ($n = 4$ in each group) of PGE$_2$- or ACSF-injected WT mice, KO;GFP+ mice and orexin neuron-ablated mice (ORX-AB). *$P < 0.05$ vs. ACSF. No orexin-immunopositive cells were detected (n.d.) in ORX-AB mice. Note that c-fos did not increase by PGE$_2$ in the medial hypothalamus of the ORX-AB mice.
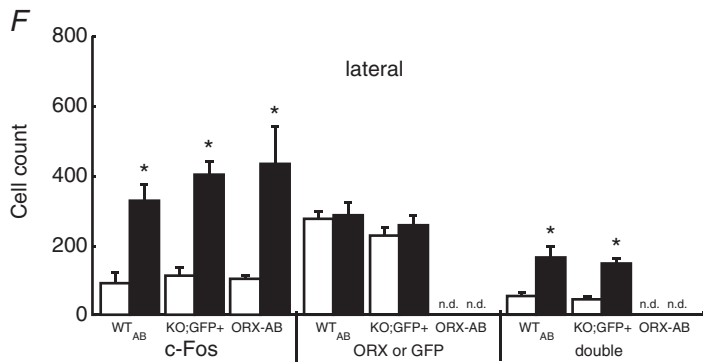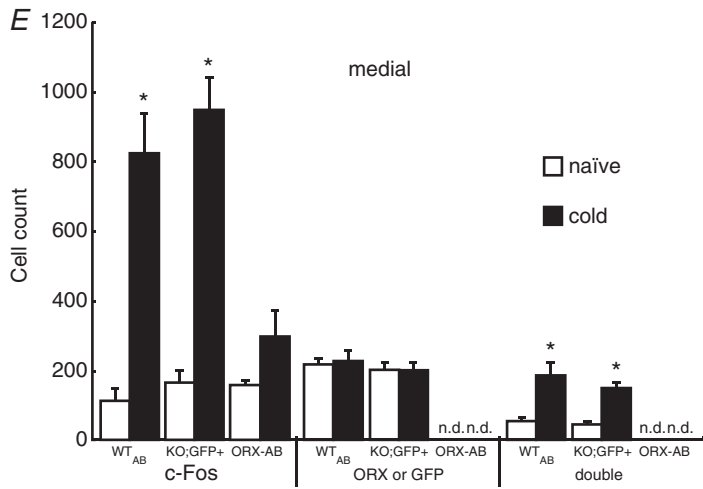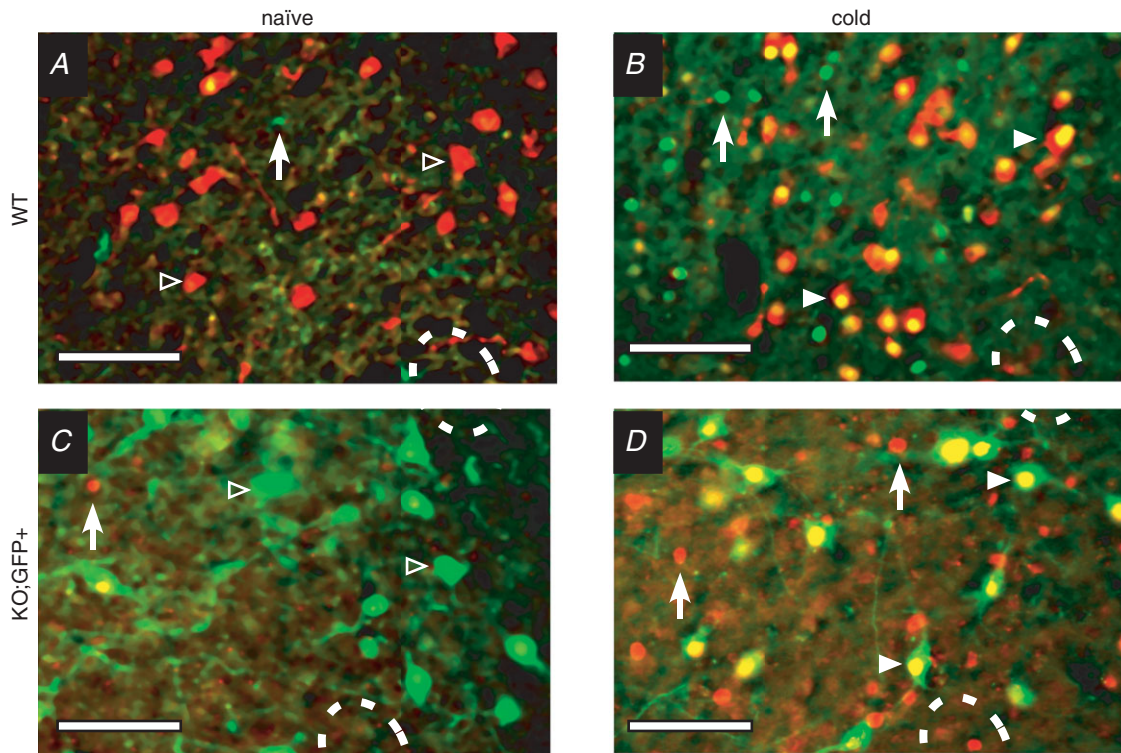
temperature to hot exposure did not differ among the three strains of mice (Fig. 4), indicating that ORX-AB mice had normal heat sensitivity. In both WT and ORX-KO mice, PGE$_2$ or cold exposure activated orexin neurons (Figs 5 and 6). In ORX-AB mice, c-fos expression in the DMH/DHA region, where many descending neurons to the raphe pallidus were located (Fig. 7), was not increased by PGE$_2$ or cold exposure. Absence of the projection from orexin neurons to the DMH/DHA neurons seemed to be at least one of the critical reasons of the abnormal thermogenesis in the ORX-AB mice. Pretreatment with the glutamate receptor antagonists, AP5 and CNQX, but not with the orexin receptor antagonists, SB334867 and OX2 29, successfully inhibited PGE$_2$-induced fever and shivering (Fig. 9). Together, these observations support the notion that orexin neurons possess a generalised importance in thermogenesis that is not restricted to stress-induced thermogenesis. In addition, these results indicate the orexin neurons can be one of the sources of glutamate transmission (Li *et al.* 2002; Schöne *et al.* 2012) in the DMH/DHA and in the raphe pallidus that is required for febrile and cold-evoked thermogenesis (Madden & Morrison, 2004; Cao & Morrison, 2006; Morrison, 2011; Morrison & Nakamura, 2011; Nakamura & Morrison, 2011).

Shivering and behavioural adjustments

In addition to body temperature and BAT temperature, we measured shivering in the anaesthetised experiments (Figs 1 and 7) and locomotor activity in unanesthetised freely moving experiments (Figs 3 and 4). Although orexin neurons, but not orexin, seemed to be involved in BAT thermogenesis and cold tolerance, orexin *per se* may be involved in PGE$_2$-induced shivering because an increase in nuchal EMG was significantly attenuated not only in ORX-AB mice, but also in ORX-KO mice (Fig. 1*C'*). However, this possibility was not confirmed

by the pharmacological experiment in which orexin receptor antagonists (SB334867 and OX2 29) did not affect shivering induced by successive intracerebroventricular injections of PGE$_2$. We do not know at present the reason for this apparent discrepancy. The limitations of the drug dosing (1 mM was the maximal concentration for SB33467 in the current experimental setup) and/or limited drug distribution in the brain might cause a negative result. These orexin receptor antagonists may not effective blockers, as suggested by Tupone *et al.* (2011). Differences in the PGE$_2$ injection methods and/or the absence/presence of artificial ventilation might also affect the result. Nevertheless, we can state that orexin neurons are important for PGE$_2$-induced shivering, in addition to BAT thermogenesis, although we do not yet know the precise neurotransmitters involved.

In addition to internal thermogenic mechanisms, we expected possible differences in the behavioural adjustments to cold environments between ORX-AB and WT mice because basal locomotor activity is smaller in ORX-AB than in WT mice, even in a normal room temperature environment (Hara *et al.* 2001). However, the increase in locomotor activity in ORX-AB mice in response to cold exposure was similar to that in WT mice. Therefore, we conclude that cold intolerance in ORX-AB mice is not due to their behavioural differences to cold exposure.

Methodological considerations in the histological experiment

To identify orexin neurons in orexin-deficient mice, we used anti-LacZ immunostaining in our previous study, but the sensitivity of this method was relatively low ($\sim$10% of orexin neurons were positive for LacZ) (Zhang *et al.* 2010). Therefore, we used ORX-KO;ORX-GFP mice instead of ORX-KO mice in this study. They were the offspring

**Figure 6. Immunohistochemical evidence for activation of orexin neurons by cold exposure**
A and *B*, representative photographs of double immunostaining for orexin and c-fos in the hypothalamus of a naïve WT mouse (*A*) and of a WT mouse exposed to a cold (5°C) environment for 60 min (*B*). Orexin is stained in red, c-fos in green. Yellow designates cells stained for both orexin and c-fos. Filled triangles indicate double-stained cells, and open triangles indicate orexin-containing but not c-fos-expressing cells. Arrows indicate c-fos in non-orexin cells. *C* and *D*, representative photographs of immunostaining for c-fos in the hypothalamus of orexin-knockout (KO) mice that carries the orexin neuron-specific expression of green fluorescent protein (KO;GFP+). Brains were sampled from a naïve mouse (*C*) and from a mouse exposed to a cold (5°C) environment for 60 min (*D*). c-fos is stained in red. Yellow designates cells that possess GFP and are stained for c-fos. Filled triangles indicate double-labelled cells, and open triangles indicate GFP-containing but not c-fos-expressing cells. Arrows indicate c-fos in non-orexin cells. Bar = 100 μm. Hypothalamic sections were immunostained for orexin and c-fos, as described in the Methods and in the legend to Fig. 5. *E* and *F*, bar graphs showing the numbers of c-fos-immunopositive cells, orexin (ORX) or GFP-containing cells, and double-labelled cells (c-fos and ORX in WT, and c-fos and GFP in KO) in the medial (*E*) and lateral (*F*) part of the hypothalamus (see Fig. 5*E* for definition of the medial and lateral part). Data are presented as mean ± SEM ($n = 4$ in each group) of naïve or cold-exposed WT mice, KO;GFP+ mice and ORX-AB mice. *$P < 0.05$ *vs.* naïve. No orexin-immunopositive cells were detected (n.d.) in ORX-AB mice. Note that c-fos did not increase by cold exposure in the medial hypothalamus of the ORX-AB mice.

from the crossing of ORX-KO mice and ORX-GFP mice, of which the latter express enhanced GFP exclusively in orexin neurons under the control of the human orexin promoter (Yamanaka *et al.* 2003). As expected, we found ~400 GFP-positive cells in the hypothalamus of the ORX-KO;ORX-GFP mice, which corresponds to about 80% of orexin neurons in the WT mice (~500 per mouse). In addition, an ORX-KO heterozygous mouse, which carried the ORX-GFP transgene, expressed GFP in 78% (384/495) of orexin-immunopositive cells. ORX-KO;ORX-GFP mice showed no orexin-like immunoreactivity. Importantly, ORX-KO;ORX-GFP mice showed a similar phenotype to that seen in ORX-KO mice. The rectal temperature in the ORX-KO;ORX-GFP mice increased by $3.7 \pm 0.3°C$ ($n = 4$) at 30 min after the intracerebroventricular injection of PGE_2. This value corresponds well to the $3.5 \pm 0.2°C$ ($n = 8$) found in ORX-KO mice (Fig. 2), although the rectal temperature

in the histological experiment was obtained by a spot measurement using a rectal temperature probe, while the body temperature in ORX-KO mice was continuously measured by an indwelling telemeter. Therefore, we conclude that ORX-KO;ORX-GFP mice are good substitutes for ORX-KO mice, and they allow for the reliable and easy identification of orexin neurons.

Possible reason for abnormal thermoregulation in ORX-AB mice

BAT morphology in ORX-KO mice and ORX-AB mice was normal in this study (Fig. 8). Although Sellayah *et al.* (2011) reported malformation of the BAT in ORX-KO mice, they used an ORX-KO homozygous mother to make ORX-KO pups and showed that maternal orexin injections during pregnancy rescued the defect. We used ORX-KO heterozygous parents to make ORX-KO
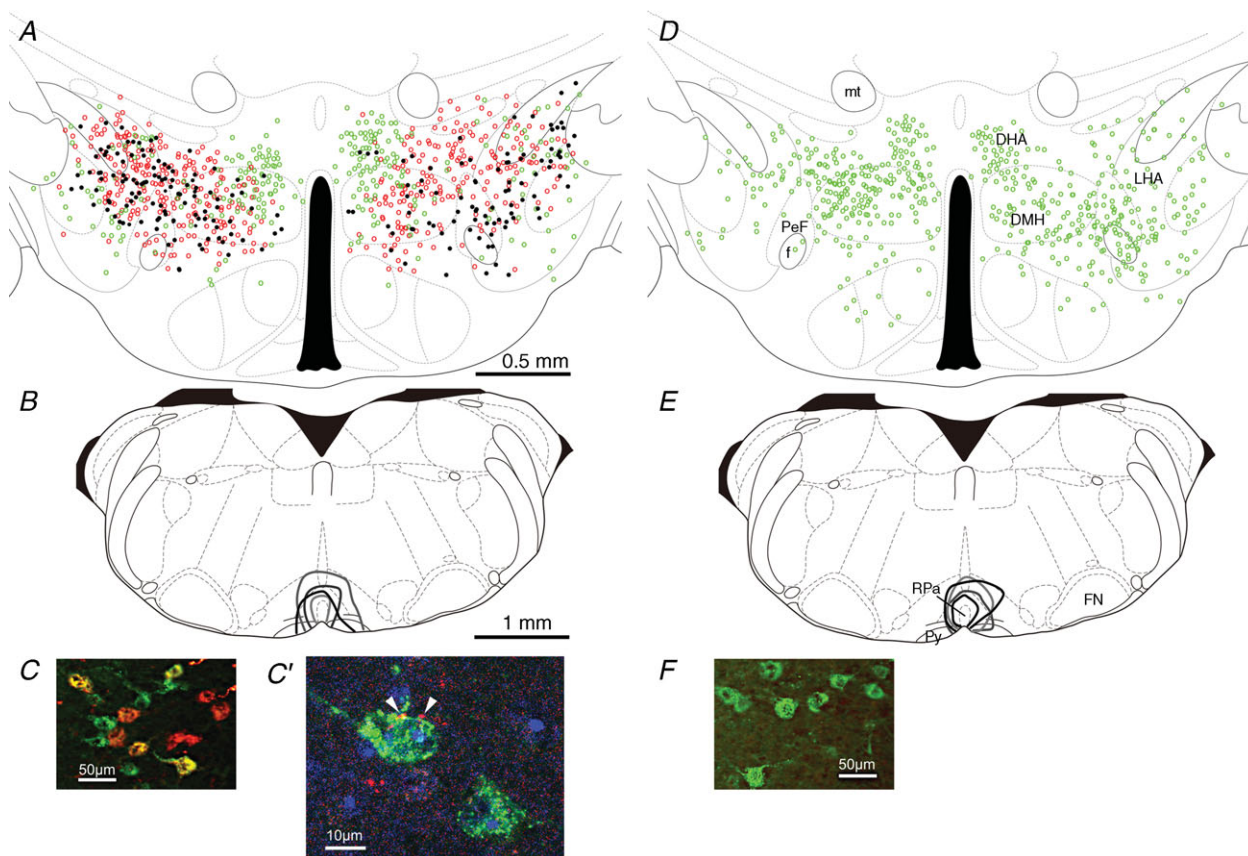
Figure 7. Distribution of retrogradely labelled neurons in the hypothalamus following cholera toxin b subunit injection into the rostral raphe pallidus
Schematic diagrams in *A* and *D* show locations of cholera toxin subunit b (CTb)-containing (green circles), orexin-immunoreactive (red circles) and double-labelled (black dots) neurons following CTb injection into the rostral raphe pallidus (RPa) (*B* and *E*) of wild-type mice (*A–C*) and orexin neuron-ablated mice (*D–F*). Results in four animals (one typical specimen per animal) were plotted on an atlas drawing. *C* and *F*, representative photographs in WT mice and orexin neuron-ablated mice, respectively. *C′*, of orexin-immunoreactive nerve terminals (arrow) attaching to the CTb-positive cell found in the dorsal hypothalamic area (DHA) in a wild-type mouse. DMH, dorsomedial hypothalamus; f, fornix; FN, facial nucleus; LHA, lateral hypothalamic area; mt, mammillary tract; PeF, perifornical area; Py, pyramidal tract.

homozygous pups and a WT mother to make ORX-AB transgenic mice. Therefore, there is no discrepancy between the reports. In addition, we have previously shown that pharmacological activation with a $\beta 3$ agonist, CL316243, resulted in a normal increase of BAT temperature in both ORX-KO mice and ORX-AB mice (Zhang *et al.* 2010). Therefore, abnormal thermo-regulation in ORX-AB mice is probably attributable to abnormalities in the brain.

The thermoregulatory system in the brain can be divided into sensory and motor output pathways. As c-fos expression in the lateral hypothalamic area of the ORX-AB mice was comparable to those in WT mice (Figs 5 and 6), sensory input to the hypothalamus appeared to be largely diminished. These results suggest the probable participation of orexin neurons in the thermogenic output pathways.

Location of the orexin neurons in the thermoregulatory circuit

There seemed to be two possibilities for the location of the orexin neurons in the PGE$_2$- and cold exposure-induced thermogenic pathways. One is that some of the orexin neurons *per se* function as a part of DMH/DHA-raphe thermogenic neurons (Oldfield *et al.* 2002; Cano *et al.* 2003; Berthoud *et al.* 2005; DiMicco & Zaretsky, 2007; Tupone *et al.* 2011). In fact, some orexin neurons located in the DMH and perifornical/LHA regions send descending projection to the raphe pallidus in rats (Tupone *et al.* 2011) and mice (Fig 7 in this experiment). Although we expected a decreased number of CTb-positive cells in the ORX-AB mice, it was comparable to that in the WT mice.
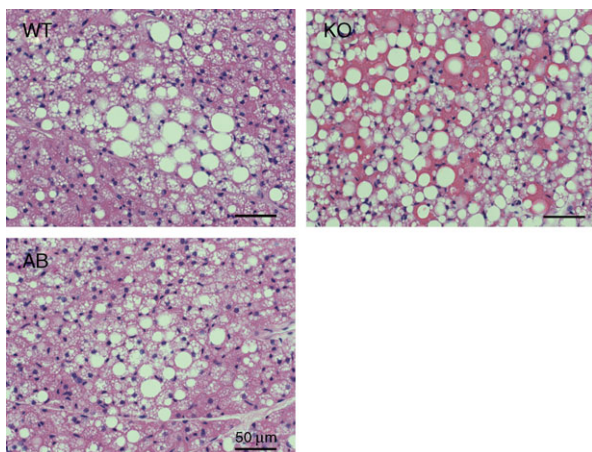
Figure 8. Apparently normal morphology of the brown adipose tissue in mutant mice
Intrascapular brown adipose tissues were excised, thin sectioned in paraffin, and stained with haematoxylin and eosin. No apparent reduction in intracellular lipids was observed in orexin-knockout mice (KO) or orexin neuron-ablated mice (AB) as compared with wild-type mice (WT) ($n = 4$, each). Representative images are shown.

One possible explanation is that the number of CTb- and orexin-double positive cells ($\sim$60 per animal) was so small that we might not be able to detect a possible change in the whole CTb-positive population ($\sim$700). In addition, compensatory changes may occur in the ORX-AB mice.

Another possibility is that some orexin neurons provide tonic excitation to the DMH/DHA-raphe thermogenic neurons through their projection to the DMH/DHA (Peyron *et al.* 1998). We confirmed that orexin-containing nerve terminals make apposition to some CTb-positive (having putative descending projection to the raphe pallidus) DHA neurons (Fig 7C'). When tonic inhibition from the preoptic area to the DMH/DHA is disinhibited by cold exposure or PGE$_2$ (Rathner *et al.* 2008; Yoshida *et al.* 2009; McAllen *et al.* 2010), this orexin neuron-dependent tonic excitation then becomes apparent in the DMH/DHA neurons. However, orexin neurons are not the sole tonic excitatory source to the DMH/DHA-raphe thermogenic neurons because PGE$_2$-induced fever occurs even in the day (resting period of nocturnal mice) or under anaesthetised conditions, both of which are known to diminish spontaneous activity of orexin neurons (Mileykovskiy *et al.* 2005; Takahashi *et al.* 2008). Note, however, that the application of the same dose of PGE$_2$ through the same injection route induced a larger temperature increase when the animals were awake (Fig. 2) than when they are anaesthetised (Fig. 9). This observation coincides well with the above-mentioned orexin neuron-dependent tonic excitatory hypothesis.

Both the direct projection to the raphe pallidus and the indirect projection through DMH/DHA from orexin neurons were eliminated in ORX-AB mice. We cannot estimate the relative importance of these pathways based on the current results. However, it should be emphasised that elimination of both pathways resulted in almost complete loss of febrile and cold-evoked thermogenesis.

Possible neurotransmitter/modulators in the orexin neurons for PGE$_2$-induced fever and cold defence

The pharmacological experiment indicated the possible involvement of glutamate receptors in PGE$_2$-induced thermogenesis. However, this experiment had three major limitations. First, excitation of the orexin neurons would be indirect because there is no report showing the existence of EP3 receptors, a fever-related subtype of PGE2 receptors, on the orexin neurons. Even if PGE$_2$ had been injected into the preoptic area, where EP3 receptors are abundant (Nakamura *et al.* 2005), as in the experiment shown in Fig. 1, it would then activate several neurons other than the orexin neurons. To specifically excite the orexin neurons, we should use photostimulation of orexin/channelrhodopsin-transgenic mice (Adamantidis *et al.* 2007). The second limitation was the low solubility of SB334867 in ACSF. We cannot
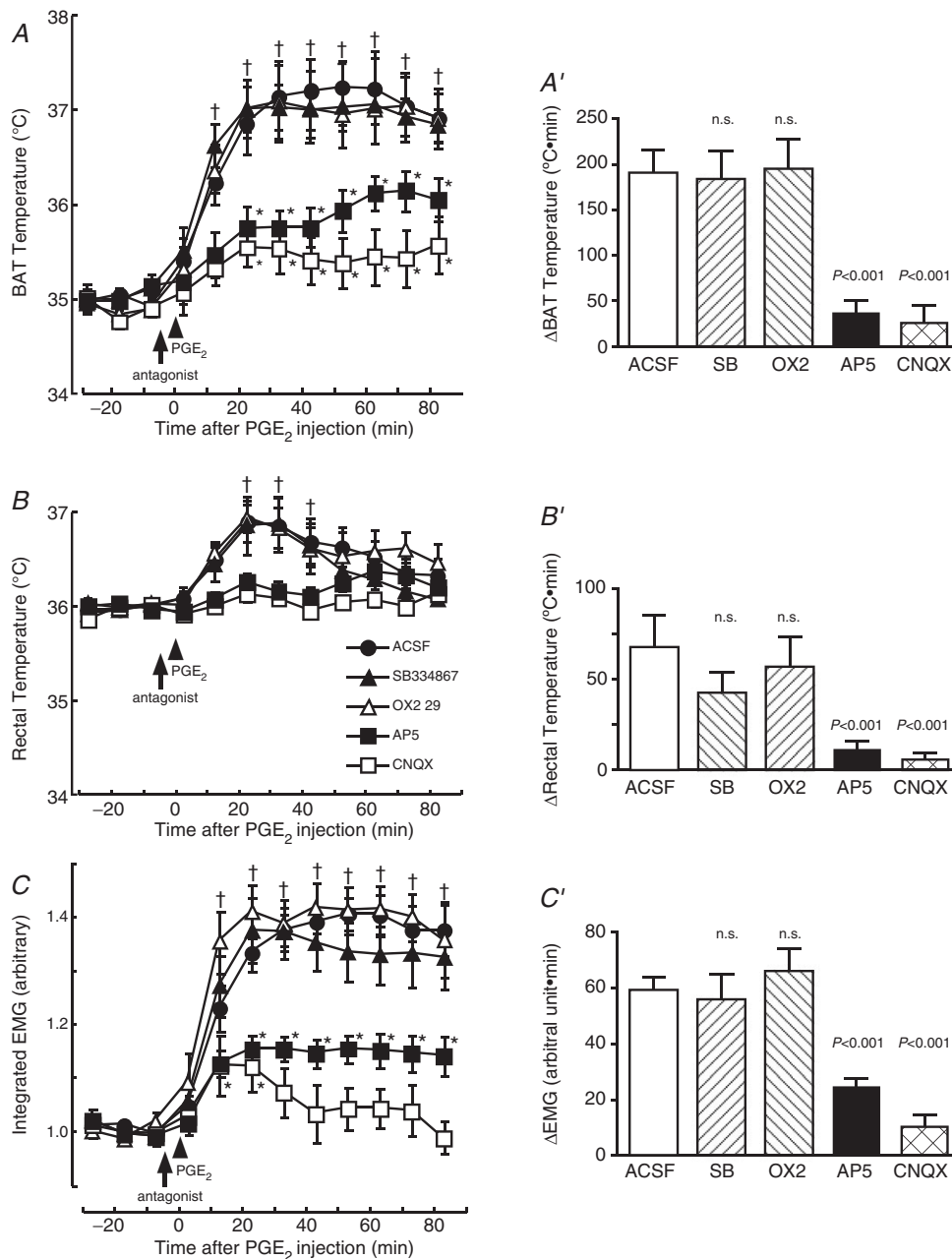
Figure 9. Effect of orexin receptor antagonists (SB334867 and OX2 29) and glutamate receptor antagonists (AP5 and CNQX) on PGE$_2$-induced fever

In chloralose (80 mg kg^{-1})/urethane (800 mg kg^{-1})-anaesthetised and artificially ventilated C57BL/6 mice, an orexin receptor antagonist, a glutamate receptor antagonist or ACSF was administered into the lateral ventricle in a volume of 2 μl at the time indicated by the arrow. After 5 min, PGE$_2$ (1 mg ml^{-1}, 2 μl) was injected into the same ventricle. Time-related changes in brown adipose tissue (BAT) temperature, rectal temperature and nuchal electromyogram (EMG, as a measure of shivering) are shown in *A*, *B* and *C*, respectively, and the changes expressed as the area under the curve above the baseline in them for 90 min are summarized in *A'*, *B'* and *C'*, respectively. Tested drugs were as follows: an orexin receptor-1-specific antagonist, SB334867 (1 mM, $n = 6$); an orexin receptor-2-specific antagonist, OX2 29 (100 mM, $n = 5$); an NMDA-selective glutamate receptor antagonist, AP5 (10 mM, $n = 8$); an AMPA/kainate-selective glutamate receptor antagonist, CNQX (10 mM, $n = 6$); and ACSF ($n = 7$). Only one drug was tested in each animal. Data are presented as mean ± SEM. *$P < 0.05$ compared with baseline value before injection of antagonist (Bonferroni's *post hoc* test). †The values in the three groups (ACSF, SB334867 and OX2 29) are significantly different ($P < 0.05$) from the corresponding baseline values. In *A'–C'*, values are compared with that of the ACSF group (ANOVA followed by Bonferroni's *post hoc* test). n.s., Not significant. Note that the glutamate receptor antagonists, but not the orexin receptor antagonists, successfully inhibited the PGE$_2$-induced fever and shivering.

exclude the possible contribution of orexin-1 receptors in PGE$_2$-induced thermoregulation because PGE$_2$-induced shivering was attenuated in ORX-KO mice (Fig. 1). Nevertheless, results from our pharmacological study (Fig. 9) support normal thermogenesis in ORX-KO mice. The third limitation was that the relatively large volume used in this experiment (two times of 2 μl, I.C.V.) might cause unspecific effects. However, we compared the effect of antagonists (SB334867, OX2 29, AP5, CNQX) with that of the same volume of vehicle (ACSF). In addition, we confirmed in our preliminary experiment that injection of ACSF plus ACSF did not cause any effect on body temperature and that injection of PGE$_2$ alone (without pretreatment) induced a similar increase of body temperature as injection of ACSF plus PGE$_2$. Therefore, we believe that our conclusion (glutamate receptor antagonists but not orexin receptor antagonists were effective) will not change when a smaller volume is used.

Although we cannot exclude the possible contribution of other co-localising substances, such as dynorphin (Chou *et al.* 2001), galanin (Hakansson *et al.* 1999) and nitric oxide (Cheng *et al.* 2003), in PGE$_2$-induced thermogenesis and cold defence, a possible contribution of glutamate is well supported in the literature. Micro-injection of glutamate receptor antagonists into the raphe pallidus inhibited the activation of BAT sympathetic nerves that were evoked by stimulation of DMH/DHA (Cao & Morrison, 2006), by PGE2 (Madden & Morrison, 2003) and by cold exposure (Nakamura & Morrison, 2007). Microinjection of a non-selective glutamate receptor antagonist, kynurenate, into the DMH/DHA inhibited BAT sympathetic activation evoked by PGE$_2$ into the preoptic area (Madden & Morrison, 2004). On the other hand, dynorphin (Handler *et al.* 1994) and nitric oxide (Steiner *et al.* 2002) within the brain have been suggested as thermolytic. Nevertheless, it should be clarified whether glutamate in the orexin neurons actually contributes to the thermogenic responses.

References

Abrahamson EE, Leak RK & Moore RY (2001). The suprachiasmatic nucleus projects to posterior hypothalamic arousal systems. *Neuroreport* **12**, 435–440.

Adamantidis AR, Zhang F, Aravanis AM, Deisseroth K & de Lecea L (2007). Neural substrates of awakening probed with optogenetic control of hypocretin neurons. *Nature* **450**, 420–424.

Arrigoni E, Mochizuki T & Scammell TE (2010). Activation of the basal forebrain by the orexin/hypocretin neurons. *Acta Physiol* **198**, 223–235.

Berthoud H-R, Patterson LM, Sutton GM, Morrison C & Zheng H (2005). Orexin inputs to caudal raphé neurons involved in thermal, cardiovascular, and gastrointestinal regulation. *Histochem Cell Biol* **123**, 147–156.

Cano G, Passerin AM, Schiltz JC, Card JP, Morrison SF & Sved AF (2003). Anatomical substrates for the central control of sympathetic outflow to interscapular adipose tissue during cold exposure. *J Comp Neurol* **460**, 303–326.

Cao W-H & Morrison SF (2006). Glutamate receptors in the raphe pallidus mediate brown adipose tissue thermogenesis evoked by activation of dorsomedial hypothalamic neurons. *Neuropharmacology* **51**, 426–437.

Chemelli RM, Willie JT, Sinton CM, Elmquist JK, Scammell T, Lee C, Richardson JA, Williams SC, Xiong Y, Kisanuki Y, Fitch TE, Nakazato M, Hammer RE, Saper CB & Yanagisawa M (1999). Narcolepsy in orexin knockout mice: molecular genetics of sleep regulation. *Cell* **98**, 437–451.

Cheng SB, Kuchiiwa S, Gao HZ, Kuchiiwa T & Nakagawa S (2003). Morphological study of orexin neurons in the hypothalamus of the Long-Evans rat, with special reference to co-expression of orexin and NADPH-diaphorase or nitric oxide synthase activities. *Neurosci Res* **46**, 53–62.

Chou TC, Lee CE, Lu J, Elmquist JK, Hara J, Willie JT, Beuckmann CT, Chemelli RM, Sakurai T, Yanagisawa M, Saper CB & Scammell TE (2001). Orexin (hypocretin) neurons contain dynorphin. *J Neurosci* **21**, RC168.

Conte WL, Kamishina H & Reep RL (2009). Multiple neuroanatomical tract-tracing using fluorescent Alexa Fluor conjugates of cholera toxin subunit B in rats. *Nature Protocols* **4**, 1157–1166.

Deng B-S, Nakamura A, Zhang W, Yanagisawa M, Fukuda Y & Kuwaki T (2007). Contribution of orexin in hypercapnic chemoreflex: evidence from genetic and pharmacological disruption and supplementation studies in mice. *J Appl Physiol* **103**, 1772–1779.

DiMicco JA & Zaretsky DV (2007). The dorsomedial hypothalamus: a new player in thermoregulation. *Am J Physiol Regul Integr Comp Physiol* **292**, R47–63.

Elias CF, Saper CB, Maratos-Flier E, Tritos NA, Lee C, Kelly J, Tatro JB, Hoffman GE, Ollmann MM, Barsh GS, Sakurai T, Yanagisawa M & Elmquist JK (1998). Chemically defined projections linking the mediobasal hypothalamus and the lateral hypothalamic area. *J Comp Neurol* **402**, 442–459.

Estabrooke IV, McCarthy MT, Ko E, Chou TC, Chemelli RM, Yanagisawa M, Saper CB & Scammell TE (2001). Fos expression in orexin neurons varies with behavioral state. *J Neurosci* **21**, 1656–1662.

Fadel J, Bubser M & Deutch AY (2002). Differential activation of orexin neurons by antipsychotic drugs associated with weight gain. *J Neurosci* **22**, 6742–6746.

Hakansson M, de Lecea L, Sutcliffe JG, Yanagisawa M & Meister B (1999). Leptin receptor- and STAT3-immunoreactivities in hypocretin/orexin neurones of the lateral hypothalamus. *J Neuroendocrinol* **11**, 653–663.

Handler CM, Piliero TC, Geller EB & Adler MW (1994). Effect of ambient temperature on the ability of mu-, kappa- and delta-selective opioid agonists to modulate thermoregulatory mechanisms in the rat. *J Pharmacol Exp Ther* **268**, 847–855.

Hara J, Beuckmann CT, Nambu T, Willie JT, Chemelli RM, Sinton CM, Sugiyama F, Yagami K, Goto K, Yanagisawa M & Sakurai T (2001). Genetic ablation of orexin neurons in mice results in narcolepsy, hypophagia, and obesity. *Neuron* **30**, 345–354.

Harris GC, Wimmer M & Aston-Jones G (2005). A role for lateral hypothalamic orexin neurons in reward seeking. *Nature* **437**, 556–559.

Kayaba Y, Nakamura A, Kasuya Y, Ohuchi T, Yanagisawa M, Komuro I, Fukuda Y & Kuwaki T (2003). Attenuated defense response and low basal blood pressure in orexin knockout mice. *Am J Physiol Regul Integr Comp Physiol* **285**, R581–593.

Li Y, Gao X-B, Sakurai T & Pol ANvd (2002). Hypocretin/orexin excites hypocretin neurons via a local glutamate neuron – a potential mechanism for orchestrating the hypothalamic arousal system. *Neuron* **36**, 1169–1181.

Madden CJ & Morrison SF (2003). Excitatory amino acid receptor activation in the raphe pallidus area mediates prostaglandin-evoked thermogenesis. *Neuroscience* **122**, 5–15.

Madden CJ & Morrison SF (2004). Excitatory amino acid receptors in the dorsomedial hypothalamus mediate prostaglandin-evoked thermogenesis in brown adipose tissue. *Am J Physiol Regul Integr Comp Physiol* **286**, R320–325.

McAllen RM, Tanaka M, Ootsuka Y & McKinley MJ (2010). Multiple thermoregulatory effectors with independent central controls. *Eur J Appl Physiol* **109**, 27–33.

Mileykovskiy BY, Kiyashchenko LI & Siegel JM (2005). Behavioral correlates of activity in identified hypocretin/orexin neurons. *Neuron* **46**, 787–798.

Morrison SF (2011). Central neural pathways for thermoregulatory cold defense. *J Appl Physiol* **110**, 1137–1149.

Morrison SF & Nakamura K (2011). Central neural pathways for thermoregulation. *Front Biosci* **16**, 74–104.

Nakamura K (2011). Central circuitries for body temperature regulation and fever. *Am J Physiol Regul Integr Comp Physiol* **301**, R1207–1228.

Nakamura K & Morrison SF (2007). Central efferent pathways mediating skin cooling-evoked sympathetic thermogenesis in brown adipose tissue. *Am J Physiol Regul Integr Comp Physiol* **292**, R127–136.

Nakamura K & Morrison SF (2011). Central efferent pathways for cold-defensive and febrile shivering. *J Physiol* **589**, 3641–3658.

Nakamura Y, Nakamura K, Matsumura K, Kobayashi S, Kaneko T & Morrison SF (2005). Direct pyrogenic input from prostaglandin EP3 receptor-expressing preoptic neurons to the dorsomedial hypothalamus. *Eur J Neurosci* **22**, 3137–3146.

Nambu T, Sakurai T, Mizukami K, Hosoya Y, Yanagisawa M & Goto K (1999). Distribution of orexin neurons in the adult rat brain. *Brain Res* **827**, 243–260.

Oldfield BJ, Giles ME, Watson A, Anderson C, Colvill LM & Mckinley MJ (2002). The neurochemical characterisation of hypothalamic pathways projecting polysynaptically to brown adipose tissue in the rat. *Neuroscience* **110**, 515–526.

Paxinos G & Franklin KBJ (2001). *The Mouse Brain in Stereotaxic Coordinates*, 2nd edn. Academic Press, Tokyo.

Peyron C, Tighe DK, van den Pol AN, de Lecea L, Heller HC, Sutcliffe JG & Kilduff TS (1998). Neurons containing hypocretin (orexin) project to multiple neuronal systems. *J Neurosci* **18**, 9996–10015.

Rathner J, Madden C & Morrison S (2008). Central pathway for spontaneous and prostaglandin E2-evoked cutaneous vasoconstriction. *Am J Physiol Regul Integr Comp Physiol* **295**, R343–354.

Rosin DL, Weston MC, Sevigny CP, Stornetta RL & Guyenet PG (2003). Hypothalamic orexin (hypocretin) neurons express vesicular glutamate transporters VGLUT1 or VGLUT2. *J Comp Neurol* **465**, 593–603.

Rusyniak DE, Zaretskya DV, Zaretskaiaa MV & DiMiccob JA (2011). The role of orexin-1 receptors in physiologic responses evoked by microinjection of PgE2 or muscimol into the medial preoptic area. *Neurosci Lett* **498**, 162–166.

Sakurai T (2007). The neural circuit of orexin (hypocretin): maintaining sleep and wakefulness. *Nat Rev Neurosci* **8**, 171–181.

Sakurai T, Amemiya A, Ishii M, Matsuzaki I, Chemelli RM, Tanaka H, Williams SC, Richarson JA, Kozlowski GP, Wilson S, Arch JR, Buckingham RE, Haynes AC, Carr SA, Annan RS, McNulty DE, Liu WS, Terrett JA, Elshourbagy NA, Bergsma DJ & Yanagisawa M (1998). Orexins and orexin receptors: a family of hypothalamic neuropeptides and G protein-coupled receptors that regulate feeding behaviour. *Cell* **92**, 573–585.

Samuels BC, Zaretsky DV & DiMicco JA (2004). Dorsomedial hypothalamic sites where disinhibition evokes tachycardia correlate with location of raphe-projecting neurons. *Am J Physiol Regul Integr Comp Physiol* **287**, R472–478.

Schöne C, Cao ZFH, Apergis-Schoute J, Adamantidis A, Sakurai T & Burdakov D (2012). Optogenetic probing of fast glutamatergic transmission from hypocretin/orexin to histamine neurons in situ. *J Neurosci* **32**, 12437–12443.

Sellayah D, Bharaj P & Sikder D (2011). Orexin is required for brown adipose tissue development, differentiation, and function. *Cell Metab* **14**, 478–490.

Steiner AA, Antunes-Rodrigues J, McCann SM & Branco LG (2002). Antipyretic role of the NO-cGMP pathway in the anteroventral preoptic region of the rat brain. *Am J Physiol Regul Integr Comp Physiol* **282**, R584–593.

Sunanaga J, Deng BS, Zhang W, Kanmura Y & Kuwaki T (2009). CO_2 activates orexin-containing neurons in mice. *Respir Physiol Neurobiol* **166**, 184–186.

Takahashi K, Lin JS & Sakai K (2008). Neuronal activity of orexin and non-orexin waking-active neurons during wake–sleep states in the mouse. *Neuroscience* **153**, 860–870.

Terada J, Nakamura A, Zhang W, Yanagisawa M, Kuriyama T, Fukuda Y & Kuwaki T (2008). Ventilatory long-term facilitation in mice can be observed both during sleep and wake periods and depends on orexin. *J Appl Physiol* **104**, 499–507.

Torrealba F, Yanagisawa M & Saper CB (2003). Colocalization of orexin A and glutamate immunoreactivity in axon terminals in the tuberomammillary nucleus in rats. *Neuroscience* **119**, 1033–1044.

Toyama S, Sakurai T, Tatsumi K & Kuwaki T (2009). Attenuated phrenic long-term facilitation in orexin neuron-ablated mice. *Respir Physiol Neurobiol* **168**, 295–302.

Tupone D, Madden CJ, Cano G & Morrison SF (2011). An orexinergic projection from perifornical hypothalamus to raphe pallidus increases rat brown adipose tissue thermogenesis. *J Neurosci* **31**, 15944–15955.

Vinkers CH, Groenink L, van Bogaert MJV, Westphal KGC, Kalkman CJ, van Oorschot R, Oosting RS, Olivier B & Korte SM (2009). Stress-induced hyperthermia and infection-induced fever: two of a kind? *Physiol Behav* **98**, 37–43.

Watanabe S, Kuwaki T, Yanagisawa M, Fukuda Y & Shimoyama M (2005). Persistent pain and stress activate pain-inhibitory orexin pathways. *Neuroreport* **16**, 5–8.

Yamanaka A, Beuckmann CT, Willie JT, Hara J, Tsujino N, Mieda M, Tominaga M, Yagami K, Sugiyama F, Goto K, Yanagisawa M & Sakurai T (2003). Hypothalamic orexin neurons regulate arousal according to energy balance in mice. *Neuron* **38**, 701–713.

Yoshida K, Li X, Cano G, Lazarus M & Saper CB (2009). Parallel preoptic pathways for thermoregulation. *J Neurosci* **29**, 11954–11964.

Zhang W, Sakurai T, Fukuda Y & Kuwaki T (2006). Orexin neuron-mediated skeletal muscle vasodilation and shift of baroreflex during defense response in mice. *Am J Physiol Regul Integr Comp Physiol* **290**, R1654–1663.

Zhang W, Sunanaga J, Takahashi Y, Mori T, Sakurai T, Kanmura Y & Kuwaki T (2010). Orexin neurons are indispensable for stress-induced thermogenesis in mice. *J Physiol* **588**, 4117–4129.

Zhang W, Zhang N, Sakurai T & Kuwaki T (2009). Orexin neurons in the hypothalamus mediate cardiorespiratory responses induced by disinhibition of the amygdala and bed nucleus of the stria terminalis. *Brain Res* **1262**, 25–37.

Additional information

Competing interests

None declared.

Author contributions

Conception and design: T.K. Data collection: Y.T., W.Z., K.S., C.K., A.M., J.S. and Y.Ko. Analysis and interpretation: Y.T., W.Z., K.S., T.S., Y.Ka. and T.K. Article drafting and revisions: Y.T., W.Z. and T.K. All authors approved the final version of the manuscript, all persons designated as authors qualify for authorship, and all those who qualify for authorship are listed.

Funding

Acknowledgements